caudal vena cava immediately before the perfusion. For the preparation of brain samples, the brain hemispheres from a PBS- or Hcy-injected apoE3 mouse were homogenized in 800 μl of PBS containing a protease inhibitor mixture (Roche Applied Science, Mannheim, Germany), and then centrifuged at 13,000 × *g* at 4 °C for 15 min. The supernatant was then used for Western blot analysis.

Statistical Analyses—StatView computer software (Windows) was used for statistical analysis. The statistical significance of differences between samples was evaluated by multiple pairwise comparisons among the sets of data using analysis of variance and the Bonferroni *t* test.

RESULTS

We examined the cholesterol and PC efflux from cultured astrocytes induced by apoE3, apoE3 pretreated with Hcy, and apoE4 24 h after the commencement of treatment of apoEs at various concentrations (Fig. 1*A*). The levels of cholesterol and PC efflux induced by apoE3 were higher than those induced by apoE3 preincubated with Hcy or apoE4 at 0.1, 0.3, and 1.0 μM. Because our previous study showed that the dimer formation of apoE3 enhances apoE3 ability to release lipids (6, 10), we determined the levels of cholesterol and PC efflux and also the assembly state of apoE3 and apoE4. The levels of cholesterol and PC efflux induced by apoE3 were significantly higher than those induced by apoE4 and apoE3 pretreated with Hcy 24 h after the commencement of treatment (Fig. 1*B*). A reduced level of lipid efflux was accompanied by a reduced level of apoE3 dimers in apoE3 samples pretreated with Hcy (Fig. 1*C*, *asterisks*). ApoE4 does not form dimers owing to a lack of cysteine. In these experiments, we confirmed that Hcy at concentrations used in our study was not toxic (see supplemental Fig. 1).

These results suggest the possibility that Hcy inhibits the dimer formation of apoE3 and this may be responsible for the reduced level of lipid efflux induced by apoE3 pretreated with Hcy, because our previous studies showed that apoE serves as a lipid acceptor in an isoform-dependent manner; apoE3 induces greater HDL generation than apoE4 (6, 7, 9). It is possible to assume that the thiol in Hcy can form disulfide bonds with the thiol of cysteine residues in apoE3. To examine whether the inhibition of thiol-disulfide bonds in apoE3 dimers affects apoE3-mediated cholesterol efflux, apoE3 or apoE4 was preincubated with a thiol-reducing agent, DTT, and then dialyzed against PBS and used for the experiment to determine cholesterol efflux. The levels of cholesterol released by apoE3 were significantly greater than those released by apoE3 pretreated with Hcy or DTT at 24 h after the commencement of treatment (Fig. 1*D*). The level of cholesterol efflux induced by apoE4 was significantly lower than that induced by apoE3, and Hcy or DTT pretreatment did not affect apoE4-induced cholesterol release (Fig. 1*D*). A reduced level of lipid efflux was accompanied by a reduced level of apoE3 dimers in apoE3 samples pretreated with Hcy or DTT (Fig. 1*D*). The effects of Hcy and DTT on apoE3 dimer formation are shown in Fig. 1*E*. The levels of apoE3 dimers (Fig. 1*E*, *asterisks*) in apoE3 samples pretreated with Hcy or DTT decreased in a Hcy- or DTT-dose-dependent manner (Fig. 1*E*). These lines of evidence suggest that the lower level of HDL generated by Hcy-bound apoE3 than by intact

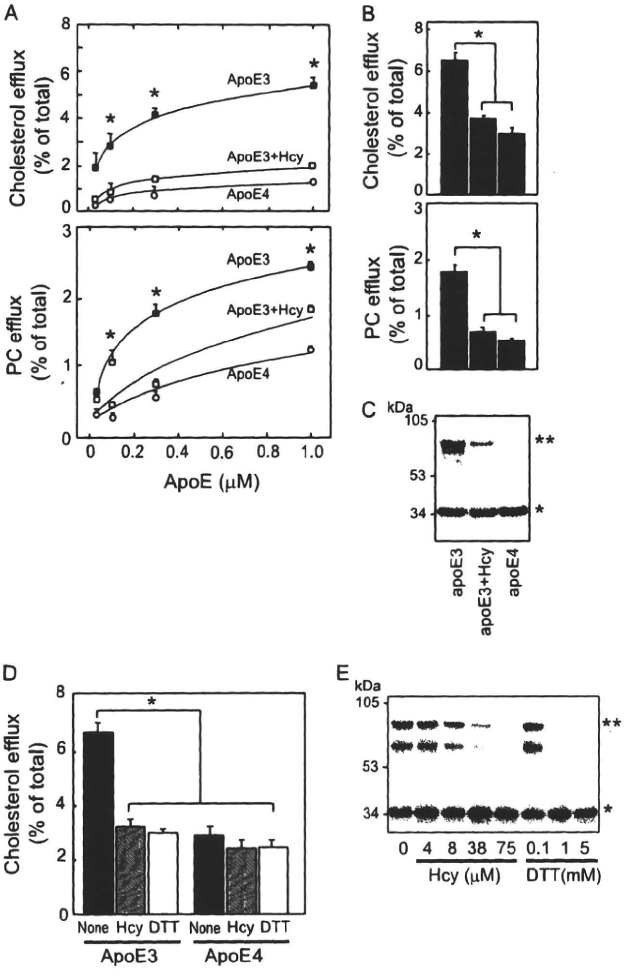

FIGURE 1. **Hcy impairs apoE3 function to generate HDL in cultured astrocytes.** *A*, the cultured astrocytes labeled with [^{14}C]acetate were exposed to apoE3 (*black squares*), apoE3+Hcy (*red squares*), and apoE4 (*yellow circles*) at 0.05, 0.01, 0.3, and 1.0 μM for 24 h. The lipids released into the media, and the lipids retained in the cells were determined. Data are means ± S.E. of four samples. *, $p < 0.001$ *versus* apoE3+Hcy and apoE4 at each dose point. The basal levels of cholesterol and PC efflux in the absence of apoEs are 1.0 ± 0.1 (%) and 0.4 ± 0.1 (%), respectively. Three independent experiments showed similar results. *B*, the percentages of released cholesterol and PC levels with respect to the total levels were calculated. Data are means ± S.E. of four samples. *, $p < 0.001$. Three independent experiments showed similar results. *C*, Western blot analysis of the samples of apoE3, apoE3+Hcy, and apoE4 was performed under nonreducing conditions. *D*, each culture was exposed to apoE3, apoE3+Hcy, apoE3+DTT, apoE4, apoE4+Hcy, and apoE4+DTT at an apoE concentration of 0.3 μM for 24 h. The percentages of released cholesterol levels with respect to the total levels were calculated. Data are means ± S.E. of four samples. *, $p < 0.001$. Three independent experiments showed similar results. *E*, Hcy at various concentrations of 4, 8, 38, and 75 μM and DTT at 0.1, 1, and 5 mM were added to the apoE3 solution, and the apoE3 solution was incubated for 24 h at 4 °C. Each solution was then dialyzed using a cassette dialyzer in PBS for 15 h at 4 °C. The apoE3-containing solutions were then analyzed by Western blot analysis under nonreducing conditions using the anti-apoE antibody (AB947). * and **, apoE3 monomers and dimers, respectively.

apoE3 results in an earlier Aβ deposition and inferior synaptic plasticity, causing earlier AD development.

We next determined whether these are also the cases for neurons. We have examined the cholesterol efflux from cultured neurons induced by apoE3, apoE3 pretreated with Hcy, apoE4, and apoE4 pretreated with Hcy at varying hours after

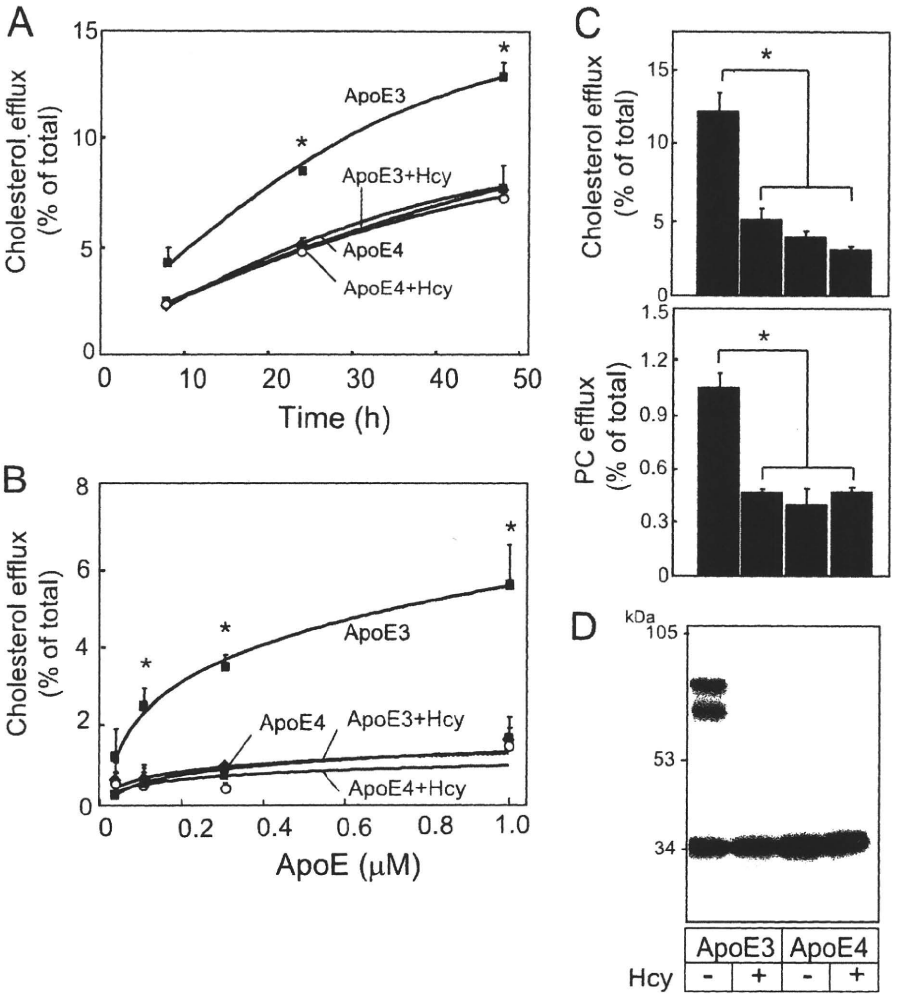

FIGURE 2. **Impairment of apoE3 function by Hcy in cultured neurons.** *A*, the cultured neurons labeled with [^{14}C]acetate were exposed to apoE3 (*blue squares*), apoE3+Hcy (*red squares*), apoE4 (*green circles*), and apoE4+Hcy (*open circles*) for various times at 0.3 μM apoE. The lipids released into the media and the lipids retained in the cells were determined. Data are means ± S.E. of four samples. *, $p < 0.001$ *versus* apoE3+Hcy, apoE4, and apoE4+Hcy at each dose point. *B*, each culture was exposed to apoE3 (*blue squares*), apoE3+Hcy (*red squares*), apoE4 (*green circles*), and apoE4+Hcy (*open circles*) at 0.05, 0.01, 0.3, and 1.0 μM for 24 h. The percentages of released cholesterol and PC levels with respect to the total levels were calculated. Data are means ± S.E. of four samples. *, $p < 0.001$. Three independent experiments showed similar results. *C*, the levels of cholesterol and PC efflux were determined in neuron cultures treated with apoE3, apoE3+Hcy, apoE4, and apoE4+Hcy 24 h after the commencement of treatment of apoEs at 0.3 μM. The percentages of released cholesterol and PC levels over the total levels were calculated. Data are means ± S.E. of four samples. *, $p <$ 0.0001. Three independent experiments showed similar results. *D*, Western blot analysis of the samples of apoE3, apoE3+Hcy, apoE4, and apoE4+Hcy was performed under nonreducing conditions.

the commencement of treatment of apoEs at 0.3 μM (Fig. 2*A*). The levels of cholesterol efflux induced by apoE3 were greater than those induced by apoE3 preincubated with Hcy, apoE4, or apoE4 preincubated with Hcy at 24 and 48 h. We also determined the levels of cholesterol efflux 24 h after the commencement of treatment of apoEs at 0.1, 0.3, and 1.0 μM (Fig. 2*B*). The levels of cholesterol efflux induced by apoE3 were greater than those induced by apoE3 preincubated with Hcy, apoE4, or apoE4 preincubated with Hcy at apoE concentrations of 0.3 and 1.0 μM. Next, we determined the levels of cholesterol and PC efflux and also the assembly state of apoE3 and apoE4. The levels of cholesterol and PC released by apoE3 were significantly greater than those released by apoE4 and by apoE3 and apoE4 pretreated with Hcy 24 h after the commencement of treatment (Fig. 2*C*). A reduced level of lipid efflux was accompanied by a reduced level of apoE3 dimers in apoE3 samples pretreated with Hcy (Fig. 2*D*). ApoE4 does not form dimers, owing to a lack of cysteine and Hcy pretreatment dis not affect the apoE4 assembly state.

Regarding the underlying molecular mechanism, we determined whether Hcy and apoE3 form disulfide bonds. We performed reverse-phase HPLC and MS of apoE3-derived peptides, LGADMEDVCGR (residues 104–114) and the Hcy-bound form of LGADMEDVCGR, namely LGADMEDVC(Hcy)GR. The HPLC profiles of the synthetic peptides LGADMEDVCGR and LGADMEDVC(Hcy)GR are shown in Fig. 3*A*, *panels a* and *b*, respectively. We also analyzed LGADMEDVCGR incubated with (Fig. 3*A*, *panel d*) or without Hcy (Fig. 3*A*, *panel c*) for 24 h at 4 °C. The LGADMEDVCGR peptides incubated with Hcy (*peaks 4* and *5*) eluted at positions corresponding to those of LGADMEDVCGR (*peak 1*) and LGADMEDVC(Hcy)GR (*peak 2*), respectively. Peaks 1–5 shown in Fig. 3*A* were analyzed by MALDI-TOF MS. A signal in peak 4 corresponds to the same molecular mass of LGADMEDVC(Hcy)GR (Fig. 3*B*, *4*) as peak 2 (Fig. 3*B*, *2*). A signal in peak 5 corresponds to the same molecular mass of LGADMEDVCGR (Fig. 3*B*, *5*) as peak 1 (Fig. 3*B*, *1*). Signals in peak 3 correspond to LGADMEDVCGR and LGADMEDVCGR dimers (Fig. 3*B*, *3*). Some of the dimers dissociate into monomers by laser irradiation during MS. These data also show that the LGADMEDVCGR peptides tend to form dimers by disulfide bonds in an environment susceptible to oxidation; however, in the presence of Hcy, Hcy inhibited the dimer formation by direct interaction with the thiol of Cys residues.

Next, we analyzed the interaction between intact apoE3 and Hcy. The solution containing intact apoE3 was incubated with or without Hcy at 4 °C for 1 day. ApoE3 in the solution was digested with trypsin, and the tryptic peptides of intact apoE3 incubated with (Fig. 3*C*, *panel e*) or without (Fig. 3*C*, *panel d*) Hcy were analyzed by HPLC. The level of peak 3 (Fig. 3*C*, *panel e*), which has the same elution time as LGADMEDVC(Hcy)GR (Fig. 3*C*, *panel b*), increased compared with that of peak 1 (Fig.

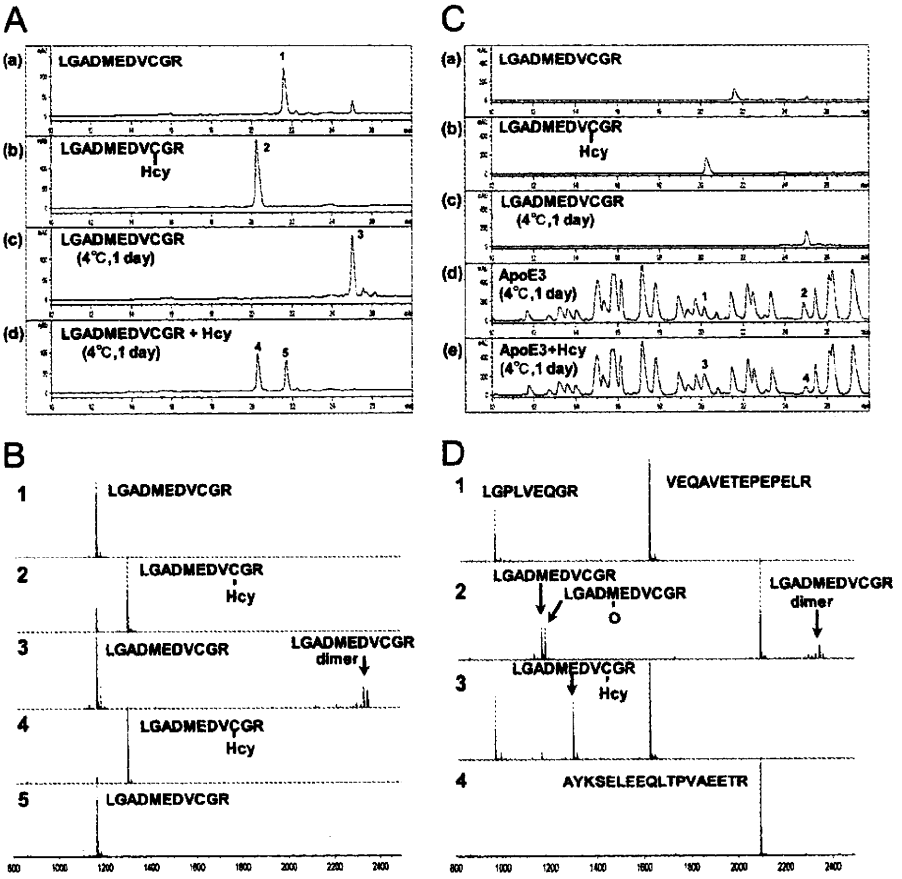

FIGURE 3. **Reverse-phase HPLC profiles and MS of apoE3-derived peptides.** *A*, LGADMEDVCGR peptides (*panel a*), LGADMEDVC(Hcy)GR peptides (*panel b*), and LGADMEDVCGR peptides incubated at 4 °C for 1 day with (*panel d*) or without (*panel c*) Hcy were subjected to HPLC. *B*, peaks 1–5 as shown in Fig. 3*A* were subjected to MALDI-TOF MS using α-cyano-4-hydroxycinnamic acid as a matrix. *C*, the tryptic peptides of intact recombinant apoE3 incubated at 4 °C for 1 day with or without Hcy were analyzed by HPLC. Elution profiles of LGADMEDVCGR (*panel a*), LGADMEDVC(Hcy)GR (*panel b*), and LGADMEDVCGR peptides incubated at 4 °C for 1 day (*panel c*), and tryptic peptides of incubated apoE3 with (*panel e*) or without (*panel d*) Hcy are shown. The elution conditions were the same as those described in *A*. *D*, *peaks 1* and *3*, which correspond to LGADMEDVC(Hcy)GR in *C*, *panel b*, and *peaks 2* and *4*, which correspond to LGADMEDVCGR dimers in Fig. 3*C*, *panel c*, were subjected to MS.

TABLE 1

The profiles of patients examined

Patient Nos. 1–6 were diagnosed as hyperhomocysteinemia and Nos. 7 to 12 were diagnosed as normal plasma Hcy. VD, vascular dementia; NPH, normal pressure hydrocephalus; SD-NFT, senile dementia of neurofibrillary tangle type; DLB, dementia with Lewy body disease; CVD, cerebrovascular disease; PSP, progressive supranuclear palsy.

No.	Age	Sex	Diagnosis	Serum Hcy	CSF Hcy
				μM	nM
1	89	F	CVD	50.4	0.90
2	75	F	CVD	1192	61.8
3	96	F	AD	45.5	1.14
4	89	F	DLB	43.8	56.2
5	71	M	PSP	25.8	0.40
6	91	F	CVD	38.0	0.6
7	81	M	VD	3.7	1.23
8	86	F	AD	5.0	0.43
9	83	F	AD	1.4	0.32
10	95	F	SD-NFT	5.7	0.32
11	84	M	NPH	6.7	0.20
12	79	M	DLB	1.9	0.22

3*C*, *panel d*), whereas that of peak 4 (Fig. 3*C*, *panel e*), which has the same elution time as LGADMEDVCGR (Fig. 3*C*, *panel c*), decreased compared with that of peak 2 (Fig. 3*C*, *panel d*).

Furthermore, peaks 1–4, shown in Fig. 3*C*, were also analyzed by MS (Fig. 3*D*). The signals in peak 1 correspond to LGPLVEQGR (residues 181–189) and VEQAVETEPEPELR (residues 2–15) (Fig. 3*D*, *peak 1*). The signals in peak 3, which has the same elution time as peak 1, correspond to LGADMEDVC(Hcy)GR, indicating that intact apoE3 binds to Hcy in addition to LGPLVEQGR and VEQAVETEPEPELR (Fig. 3*D*, *peak 3*). The signals in peak 2, which has the same elution time as peak 4, correspond to LGADMEDVCGR and LGADMEDVCGR dimer in addition to AYKSELEEQLTPVAEETR (residues 73–90) (Fig. 3*D*, *peak 2*).

Next, we examined whether the ratio of the apoE3 dimer is lower in the human subjects with hyperhomocysteinemia than in human subjects with normal Hcy. The CSF from human apoEε3/3 carriers with normal plasma Hcy and hyperhomocysteinemia were analyzed. The profiles of patients are shown in Table 1. The Hcy concentrations in the plasma and CSF from the patients with hyperhomocysteinemia were higher (mean ± S.E., 232.58 ± 191.91 μM for plasma and 20.17 ± 12.30 nM for CSF, Table 1) than those from the patients with normal plasma Hcy (4.07 ± 0.86 μM for plasma and 0.45 ± 0.16 nM for CSF, Table 1). The results of Western blot analysis of these samples under nonreducing conditions are shown in Fig. 4*A*. The band signals of apoE3 dimers and monomers were scanned by densitometry, and the ratio of the levels of dimers with respect to the level of total apoE3 was calculated. The ratio of the levels of apoE3 dimers with respect to the level of total apoE3 is significantly lower in those who have hyperhomocysteinemia (Fig. 4*B*). The CSF samples from the human subjects with hyperhomocysteinemia contain a higher level of Hcy (mean ± S.E. = 20.17 ± 12.30 nM, Table 1) compared with those from the human subjects with normal plasma Hcy (0.45 ± 0.16 nM, Table 1), suggesting that a larger amount of Hcy binds apoE3 molecules via disulfide bonds and inhibits apoE3 dimerization. The correlation between the level of Hcy and the ratio of apoE3 dimer is shown in supplemental Fig. 2. Dimer ratios tended to negatively correlate with Hcy level in CSF and serum samples, although it does not reach statistical significance (supplemental Fig. 1, *A* and *B*). This tendency for a negative correlation becomes stronger when the separately distributed data (a, b, or c) are removed. The serum lipid profiles of the patients and the correlations of the lipid

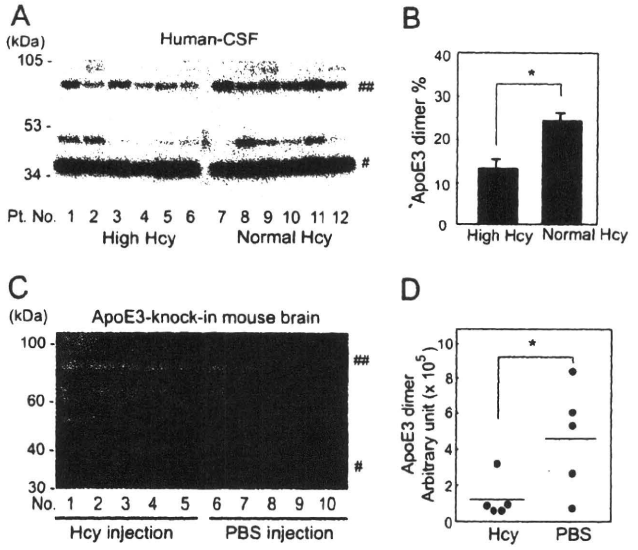

FIGURE 4. **Assembly state of apoE3 in the CSF from human subjects with normal plasma Hcy and hyperhomocysteinemia.** *A*, CSF from human subjects with hyperhomocysteinemia or normal plasma Hcy was mixed with an equal amount of sampling buffer consisting of 100 mM Tris-HCl (pH 7.4), 10% glycerol, 4% SDS, and 0.01% bromphenol blue, and analyzed using 12.5% Tris/Tricine SDS-PAGE under nonreducing conditions. The proteins transferred to the membrane were subjected to Western blot analysis using the anti-apoE antibody. # and ##, apoE3 monomers and dimers, respectively. *Pt. No.*, patient number. *B*, the ratio of signal intensities of apoE dimers with respect to total apoE (monomers plus dimers) in each sample was determined by densitometry and calculation. The values are means ± S.E. of six CSF samples from human subjects with high and normal plasma Hcy. *, $p < 0.003$. *C*, Western blot analysis of brain homogenate prepared from apoE3 knock-in mice subcutaneously injected with Hcy. *Numbers 1–5* are the samples from mice treated with Hcy, and *numbers 6–10* are those from mice treated with PBS. # and ##, the apoE3 monomers and dimers, respectively. *D*, quantification of signals representing the apoE3 dimer in *D* is determined by densitometry. The values are means ± S.E. of five brain homogenate samples. *, $p < 0.005$.

profiles and the ratio of apoE3 dimer are also shown in supplemental Table 1 and supplemental Fig. 3.

We next examined whether hyperhomocysteinemia inhibits apoE3 dimer formation in the brains of mice expressing human apoE3 without expressing rodent endogenous apoE. ApoE3 knock-in mice were injected with 100 μl of 0.6 μM Hcy subcutaneously twice a day for 6 days. The mice were then sacrificed, brains and serum were isolated, and the level of the apoE3 dimer in brain samples was determined by Western blot analysis under nonreducing conditions. The level of the apoE3 dimer in each sample that was loaded with equal amounts of brain homogenate protein is shown in Fig. 4, *C* and *D*. The Hcy level in the serum from the Hcy-injected mice is significantly higher than those from PBS-injected mice (mean ± S.E. for Hcy-treated samples is 10.26 ± 0.47 μM and that for control is 4.98 ± 0.48 μM; $p < 0.0001$). The level of the apoE3 dimer is significantly lower in Hcy-injected mouse brains than in control brains (Fig. 4*D*). Although the ratio of the apoE3 dimer in the mouse brain was very low compared with that of human CSF, these results show that a higher level of serum Hcy resulted in the attenuation of dimer formation of apoE3 in the brain.

DISCUSSION

Our previous studies have shown that intramolecular interaction (*i.e.* domain interaction) and intermolecular interaction

TABLE 2
Association of Hcy with apoE3 and apoE4

To determine the association of Hcy with apoE, 7.5 μl of 100 mM Hcy was added to 500 μl of apoE-containing solution at 14.7 mM apoE. The apoE3 and apoE4 containing solutions with or without Hcy, or Hcy solution without apoE were incubated overnight at room temperature. The solutions were then dialyzed against PBS overnight at room temperature, and the level of Hcy in each solution was determined. UD, under detectable level.

	Hcy ($n = 8$)	apoE3 ($n = 3$)	apoE4 ($n = 3$)	apoE3 + Hcy ($n = 8$)	apoE4 + Hcy ($n = 8$)
Hcy (μM)	UD	UD	UD	5.75 ± 0.25	UD

(*i.e.* dimerization) determine the apoE isoform-dependent ability to generate HDL (7, 10). Because Hcy is a molecule harboring a thiol, we hypothesized that the thiol of Hcy associates with the thiol of cysteine residues in apoE3, and the formation of this disulfide bonds interferes with apoE3 dimerization. In the present study, we found that Hcy binds to cysteine residues of apoE3, thereby interfering with apoE3 dimerization and impairing the ability of apoE3 to generate HDL to a level similar to that of apoE4. These *in vitro* results are supported by those of the analysis of human CSF samples from patients with hyperhomocysteinemia and normal serum homocysteine, showing that the ratio of the levels of apoE3 dimers with respect to the level of total apoE3 in CSF samples from patients with hyperhomocysteinemia is significantly lower than that from normal controls. In addition, the subcutaneous injection of Hcy into apoE3 knock-in mice resulted in a reduced level of the apoE3 dimer in the brain homogenate, suggesting that hyperhomocysteinemia decreases the level of apoE3 dimer in CSF or the brain.

To determine the effect of Hcy bound to apoE3, we preincubated Hcy and apoE3 at relatively high concentrations. Under these conditions, ~66% of apoE3 binds to Hcy, whereas the level of Hcy bound to apoE4 was not detected (Table 2). One may question whether the inhibitory effect of Hcy on apoE3 dimerization and apoE3-mediated lipid efflux were observed when lower concentrations of Hcy similar to those in serum or CSF were used in the presence of comparable concentrations of apoE3 in culture. Hcy at lower concentrations did not inhibit apoE3 dimerization nor attenuate apoE3-mediated lipid efflux. This may be because it takes a longer time to form disulfide bonds between Hcy and apoE3 at physiological concentrations in culture. However, this is not the case for *in vivo* conditions, including those in human CSF and the mouse brain. Although the precise mechanism underlying this discrepancy cannot be provided by the current study, the disulfide bonds between apoE3 and Hcy molecules occurs *in vivo* at concentrations lower than those used in *in vitro* experiments. In support of this notion, previous studies have shown that >70% of Hcy in plasma forms disulfide-bonded to cysteine residues of proteins including transthyretin (31, 32), suggesting that Hcy at single digit μM concentrations forms disulfide bonds to cysteine residues *in vivo*.

Previous studies have shown other biological and pathological effects of Hcy; namely, Hcy induces neuronal damage (33, 34), compromises blood-brain barrier integrity (26), modulates Aβ toxicity (35), and modulates Aβ generation (27, 28). However, the molecular mechanism(s) by which Hcy directly interacts with the molecule(s) in these studies are not fully understood. In this study, we showed that a high level of Hcy impairs

apoE3 function to a similar level of apoE4 by preventing/breaking the disulfide bonds, thereby leading to a decreased HDL generation. Because apoE-HDL plays a role in Aβ clearance(13,14), the lines of evidence suggest that two different risk factors for AD, apoE4 and hyperhomocysteinemia, may share a common mechanism; that is, apoE4 has a lower ability to generate HDL than apoE3 and the Hcy-induced modification of apoE3 impairs the ability of apoE3 to generate HDL to a level similar to that of apoE4. Our observations in the present study also provide new insight into concerning the apoE genotype-dependent treatment of hyperhomocysteinemia, especially for reducing the risk of AD.

REFERENCES

1. Strittmatter, W. J., Saunders, A. M., Schmechel, D., Pericak-Vance, M., Enghild, J., Salvesen, G. S., and Roses, A. D. (1993) *Proc. Natl. Acad. Sci. U.S.A.* **90,** 1977–1981
2. Krimbou, L., Denis, M., Haidar, B., Carrier, M., Marcil, M., and Genest, J., Jr. (2004) *J. Lipid Res.* **45,** 839–848
3. DeMattos, R. B., Brendza, R. P., Heuser, J. E., Kierson, M., Cirrito, J. R., Fryer, J., Sullivan, P. M., Fagan, A. M., Han, X., and Holtzman, D. M. (2001) *Neurochem. Int.* **39,** 415–425
4. Hara, M., Matsushima, T., Satoh, H., Iso-o, N., Noto, H., Togo, M., Kimura, S., Hashimoto, Y., and Tsukamoto, K. (2003) *Arterioscler. Thromb. Vasc. Biol.* **23,** 269–274
5. Altenburg, M., Johnson, L., Wilder, J., and Maeda, N. (2007) *J. Biol. Chem.* **282,** 7817–7824
6. Michikawa, M., Fan, Q. W., Isobe, I., and Yanagisawa, K. (2000) *J. Neurochem.* **74,** 1008–1016
7. Gong, J. S., Kobayashi, M., Hayashi, H., Zou, K., Sawamura, N., Fujita, S. C., Yanagisawa, K., and Michikawa, M. (2002) *J. Biol. Chem.* **277,** 29919–29926
8. Xu, Q., Brecht, W. J., Weisgraber, K. H., Mahley, R. W., and Huang, Y. (2004) *J. Biol. Chem.* **279,** 25511–25516
9. Gong, J. S., Morita, S. Y., Kobayashi, M., Handa, T., Fujita, S. C., Yanagisawa, K., and Michikawa, M. (2007) *Mol. Neurodegener.* **2,** 9
10. Minagawa, H., Gong, J. S., Jung, C. G., Watanabe, A., Lund-Katz, S., Phillips, M. C., Saito, H., and Michikawa, M. (2009) *J. Neurosci. Res.* **87,** 2498–2508
11. Huang, Y., Liu, X. Q., Wyss-Coray, T., Brecht, W. J., Sanan, D. A., and Mahley, R. W. (2001) *Proc. Natl. Acad. Sci. U.S.A.* **98,** 8838–8843
12. Nakamura, T., Watanabe, A., Fujino, T., Hosono, T., and Michikawa, M. (2009) *Mol. Neurodegener.* **4,** 35
13. Deane, R., Sagare, A., Hamm, K., Parisi, M., Lane, S., Finn, M. B., Holtzman, D. M., and Zlokovic, B. V. (2008) *J. Clin. Invest.* **118,** 4002–4013
14. Jiang, Q., Lee, C. Y., Mandrekar, S., Wilkinson, B., Cramer, P., Zelcer, N., Mann, K., Lamb, B., Willson, T. M., Collins, J. L., Richardson, J. C., Smith, J. D., Comery, T. A., Riddell, D., Holtzman, D. M., Tontonoz, P., and Landreth, G. E. (2008) *Neuron* **58,** 681–693
15. Kolovou, G. D., and Anagnostopoulou, K. K. (2007) *Ageing Res. Rev.* **6,** 94–108
16. McCarron, M. O., Delong, D., and Alberts, M. J. (1999) *Neurology* **53,** 1308–1311
17. Guthikonda, S., and Haynes, W. G. (1999) *Curr. Opin. Cardiol.* **14,** 283–291
18. Kim, N. K., Choi, B. O., Jung, W. S., Choi, Y. J., and Choi, K. G. (2003) *Neurology* **61,** 1595–1599
19. Perry, I. J. (1999) *J. Cardiovasc. Risk* **6,** 235–240
20. Seshadri, S., Beiser, A., Selhub, J., Jacques, P. F., Rosenberg, I. H., D'Agostino, R. B., Wilson, P. W., and Wolf, P. A. (2002) *N. Engl. J. Med.* **346,** 476–483
21. Luchsinger, J. A., Tang, M. X., Shea, S., Miller, J., Green, R., and Mayeux, R. (2004) *Neurology* **62,** 1972–1976
22. Ravaglia, G., Forti, P., Maioli, F., Martelli, M., Servadei, L., Brunetti, N., Porcellini, E., and Licastro, F. (2005) *Am. J. Clin. Nutr.* **82,** 636–643
23. Van Dam, F., and Van Gool, W. A. (2009) *Arch. Gerontol. Geriatr.* **48,** 425–430
24. Isobe, C., Murata, T., Sato, C., and Terayama, Y. (2005) *Life Sci.* **77,** 1836–1843
25. Starkebaum, G., and Harlan, J. M. (1986) *J. Clin. Invest.* **77,** 1370–1376
26. Kamath, A. F., Chauhan, A. K., Kisucka, J., Dole, V. S., Loscalzo, J., Handy, D. E., and Wagner, D. D. (2006) *Blood* **107,** 591–593
27. Pacheco-Quinto, J., Rodriguez de Turco, E. B., DeRosa, S., Howard, A., Cruz-Sanchez, F., Sambamurti, K., Refolo, L., Petanceska, S., and Pappolla, M. A. (2006) *Neurobiol. Dis.* **22,** 651–656
28. Zhang, C. E., Wei, W., Liu, Y. H., Peng, J. H., Tian, Q., Liu, G. P., Zhang, Y., and Wang, J. Z. (2009) *Am. J. Pathol.* **174,** 1481–1491
29. Hamanaka, H., Katoh-Fukui, Y., Suzuki, K., Kobayashi, M., Suzuki, R., Motegi, Y., Nakahara, Y., Takeshita, A., Kawai, M., Ishiguro, K., Yokoyama, M., and Fujita, S. C. (2000) *Hum. Mol. Genet.* **9,** 353–361
30. Michikawa, M., Gong, J. S., Fan, Q. W., Sawamura, N., and Yanagisawa, K. (2001) *J. Neurosci.* **21,** 7226–7235
31. Lim, A., Sengupta, S., McComb, M. E., Théberge, R., Wilson, W. G., Costello, C. E., and Jacobsen, D. W. (2003) *J. Biol. Chem.* **278,** 49707–49713
32. Sass, J. O., Nakanishi, T., Sato, T., Sperl, W., and Shimizu, A. (2003) *Biochem. Biophys. Res. Commun.* **310,** 242–246
33. Kruman, II, Kumaravel, T. S., Lohani, A., Pedersen, W. A., Cutler, R. G., Kruman, Y., Haughey, N., Lee, J., Evans, M., and Mattson, M. P. (2002) *J. Neurosci.* **22,** 1752–1762
34. Maler, J. M., Seifert, W., Hüther, G., Wiltfang, J., Rüther, E., Kornhuber, J., and Bleich, S. (2003) *Neurosci. Lett.* **347,** 85–88
35. White, A. R., Huang, X., Jobling, M. F., Barrow, C. J., Beyreuther, K., Masters, C. L., Bush, A. I., and Cappai, R. (2001) *J. Neurochem.* **76,** 1509–1520

Supplemental Materials

HOMOCYSTEINE, ANOTHER RISK FACTOR FOR ALZHEIMER'S DISEASE, IMPAIRS APOLIPOPROTEIN E3 FUNCTION

Hirohisa Minagawa[1)], Atsushi Watanabe[2)], Hiroyasu Akatsu[3)], Kayo Adachi[2)], Chigumi Ohtsuka[4)], Yasuo Terayama[4)], Takashi Hosono[1)], Satoshi Takahashi[4)], Hideaki Wakita[2)], Cha-Gyun Jung[1)], Hiroto Komano[5)], and Makoto Michikawa[1)]

Methods

1) Analysis of DNA fragmentation

DAN fragmentation was evaluated by FACS analysis. Astrocytes derived from mouse cortices were plated in DMEM containing 10% FBS for 72 h. The cultures were then washed three times with DMEM and cultured in a serum-free DMEM medium in the absence or presence of Hcy at various concentrations for 48 h. The cells were trypsinized and fixed in ice-cold 70% ethanol overnight at 4°C. The cells were then washed three times with PBS, stained with propidium iodide (PI, 30 mg/ml) for 30 min at room temperature and subjected to FACS analysis on a FACScan flow cytometer (BD PharMingen). Data were analyzed using the CellQuest software. For each sample, 10,000 events were collected. The percentages of DNA fragmentation reflecting apoptotic cells were determined by measuring the fraction of nuclei containing a hypodiploid DNA content (sub-G1 fraction).

2) Cell viability analysis

Cell viability was evaluated using CellTiter-Glo Luminescent Cell Viability Assay (Promega, Madison, WI, USA). Briefly, astrocytes derived from mouse cortices were seeded into 96-well plates in DMEM containing 10% FBS for 72h. The cultures were then washed three times with DMEM and cultured in a serum-free DMEM medium in the absence or presence of Hcy at various concentrations for 48 h. Cell viability was determined according to the manufacturer's instruction.

3) Correlation between levels of CSF or serum Hcy and the ratio of apoE3 dimer

The levels of Hcy in the CSF and the serum of the patients with normal serum Hcy or hyperhomocystenemia were determined as described in the Experimental Procedures in

the text. The ratio of apoE3 dimer was determined by Western blot analysis under non-reducing conditions as described in the text.

Legends

Supplemental Fig. 1

Effect of Hcy on the viability (A) and apoptosis (B) of astrocytes derived from mouse cortices. (A) Astrocytes were exposed to indicated concentrations of Hcy for 48h in serum-free DMEM. Cell viability was determined using CellTiter-Glo Luminescent Cell Viability Assay and is shown as a percentage of living cells. (B) Flow cytometry analysis was used to assess fragmentation after PI staining. Cells within the sub-G1 population contain fragmented DNA. Such cells are considered undergoing apoptosis. Data are means ± S.E. of three independent experiments. *$p<0.005$, **$p<0.001$ *vs* control.

Supplemental Fig. 2

The correlation between the level of Hcy and the ratio of apoE3 dimer is shown. (A) The level of Hcy in the CSF and the ratio of apoE3 dimer in each sample are plotted. (B) The level of Hcy in the serum and the ratio of apoE3 dimer in each sample are plotted. There is a tendency for negative correlation between the dimer ratio and Hcy value in CSF and serum samples, although it does not reach spastically significant. The tendency for these negative-correlations becomes stronger when the separately distributed data, such as a, b, or c, are removed.

Supplemental Fig. 3

The levels of total cholesterol, HDL-cholesterol, and triglyceride (TG) in plasma obtained from patients with hyperhomocysteinemia and normal Hcy are shown in Supplemental Fig. 3A. The level of plasma total cholesterol is significantly higher in patients with hyperhomocysteinemia than in normal controls. In contrast, there is no difference in the levels of HDL-cholesterol and TG between these two groups. The correlations between the ratio of apoE3 dimer and the levels of total cholesterol, HDL-cholesterol, and TG are shown in Supplemental Figs. 3B, C, and D, respectively. There is a significant negative correlation between the ratio of apoE3 dimer in CSF and the level of plasma total cholesterol (Supplemental Fig. 3B). However, there is no correlation between the ratio of apoE3 dimer and the levels of HDL-cholesterol and TG (Supplemental Figs. 3C, D). Although this study

shows that Hcy inhibits apoE3 dimerization, which impairs HDL generation, there is no difference in the level of HDL-cholesterol between the samples from patients with hyperhomocysteinemia and normal Hcy. This is because apolipoprotein AI, but not apoE, plays a major role in HDL generation in systemic circulation. There is a negative correlation between the ratio of apoE3 dimer and the level of plasma total cholesterol; however, it is unlikely that there is a cause-and-effect relationship between these two parameters. Because cholesterol metabolism in the brain is separated from that of systemic circulation by the blood-brain barrier, the cholesterol level in the plasma does not correlate with that in the brain. Thus, it is necessary to determine the lipid profile, including apoE-mediated HDL generation, in CSF in a future study.

Supplementl Figure 1
Minagawa et al

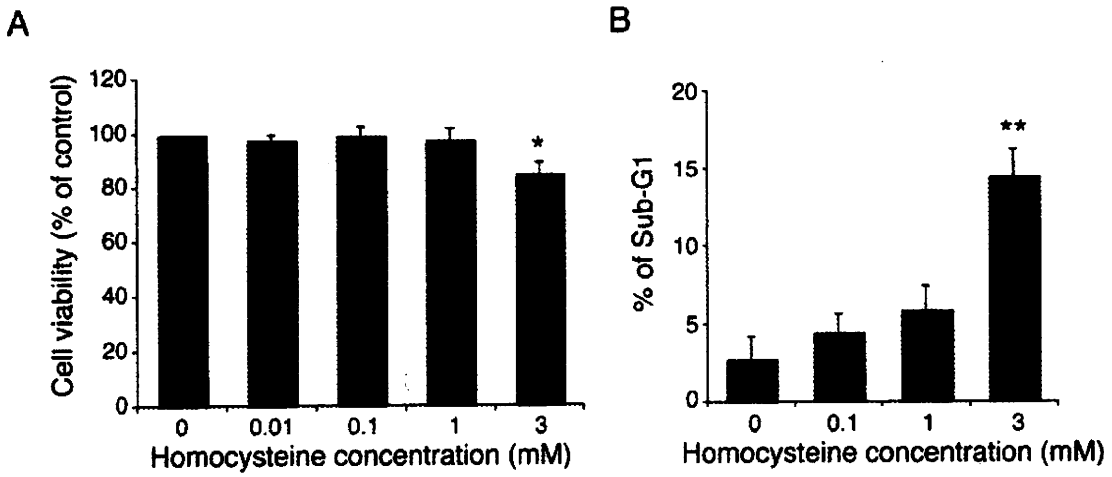

Supplemental Figure 2

Minagawa et al

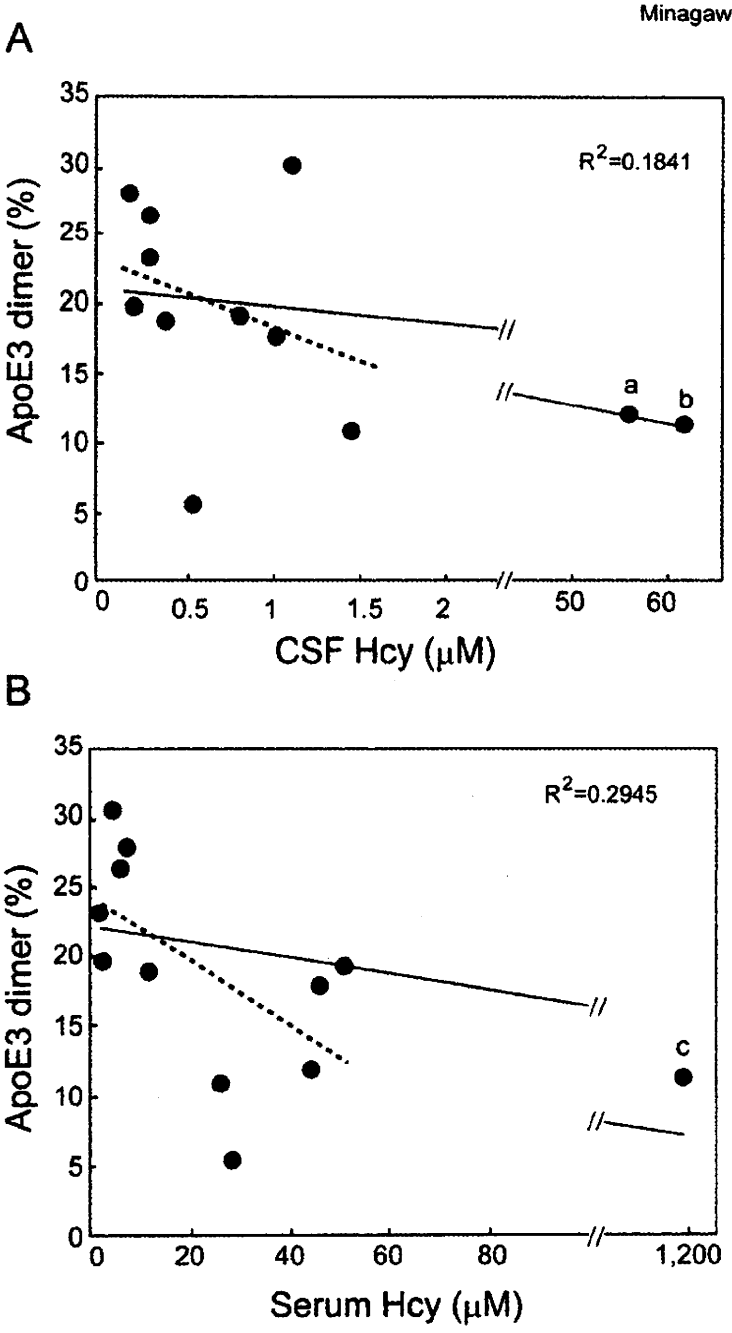

Supplemental Figure 3

Minagawa et al

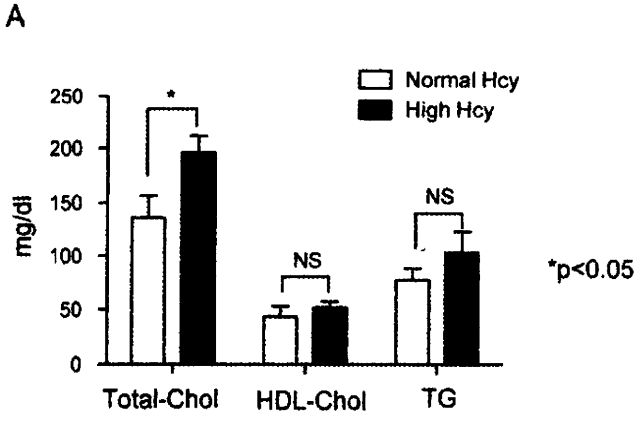

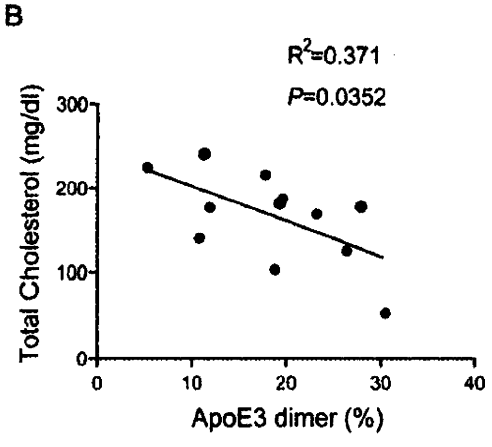

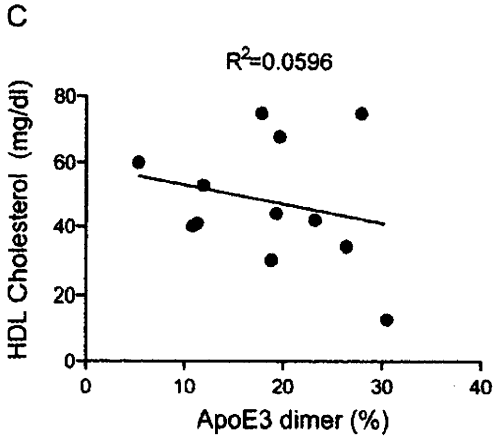

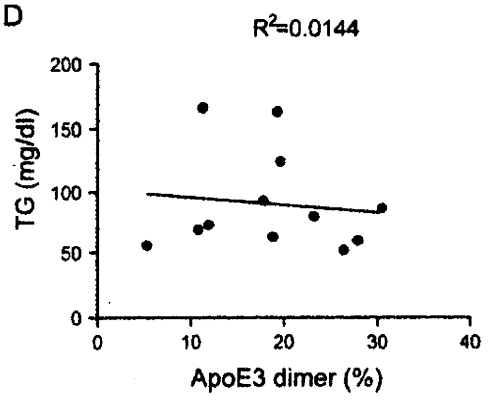

Supplemental Table 1. Plasma lipid profile of the patients

	NO	Total cholesterol (mg/dl)	HDL-cholesterol (mg/dl)	Triglyceride (mg/dl)
Normal Hcy	1	55	13	87
	2	103	30	63
	3	168	42	80
	4	124	34	52
	5	177	75	60
	6	187	68	125
High Hcy	7	176	53	73
	8	181	44	163
	9	241	41	166
	10	216	75	93
	11	139	40	69
	12	225	60	56

THE JOURNAL OF BIOLOGICAL CHEMISTRY VOL. 286, NO. 8, pp. 6393–6401, February 25, 2011

Lipoprotein Lipase Is a Novel Amyloid β (Aβ)-binding Protein That Promotes Glycosaminoglycan-dependent Cellular Uptake of Aβ in Astrocytes*[S]

Received for publication, August 4, 2010, and in revised form, November 23, 2010 Published, JBC Papers in Press, December 21, 2010, DOI 10.1074/jbc.M110.172106

Kazuchika Nishitsuji[‡], Takashi Hosono[‡], Kenji Uchimura[‡§], and Makoto Michikawa[‡1]

From the [§]Section of Pathophysiology and Neurobiology, [‡]Department of Alzheimer's Disease Research, National Center for Geriatrics and Gerontology, Obu, Aichi 474-8511, Japan

Lipoprotein lipase (LPL) is a member of a lipase family known to hydrolyze triglyceride molecules in plasma lipoprotein particles. LPL also plays a role in the binding of lipoprotein particles to cell-surface molecules, including sulfated glycosaminoglycans (GAGs). LPL is predominantly expressed in adipose and muscle but is also highly expressed in the brain where its specific roles are unknown. It has been shown that LPL is colocalized with senile plaques in Alzheimer disease (AD) brains, and its mutations are associated with the severity of AD pathophysiological features. In this study, we identified a novel function of LPL; that is, LPL binds to amyloid β protein (Aβ) and promotes cell-surface association and uptake of Aβ in mouse primary astrocytes. The internalized Aβ was degraded within 12 h, mainly in a lysosomal pathway. We also found that sulfated GAGs were involved in the LPL-mediated cellular uptake of Aβ. Apolipoprotein E was dispensable in the LPL-mediated uptake of Aβ. Our findings indicate that LPL is a novel Aβ-binding protein promoting cellular uptake and subsequent degradation of Aβ.

Lipoprotein lipase (LPL)[2] catalyzes the hydrolysis of triacylglycerol and mediates the cellular uptake of lipoproteins by functioning as a "bridging molecule" between lipoproteins and sulfated glycosaminoglycans (GAGs) or lipoprotein receptors in blood vessels (1, 2). Sulfated GAGs are side chains of proteoglycans normally found in the extracellular matrix and on the cell surface in the peripheral tissues and brain. Sulfation modifications vary within the GAG chains and are crucial for interaction between GAGs and various protein ligands (3), including LPL (4, 5).

It has been shown that LPL is distributed in numerous organs and is highly expressed in the brain (6, 7). Although the catabolic activity of LPL on triacylglycerol is observed in the brain (8), the finding that apolipoprotein CII (apoCII), an essential cofactor for LPL, is not expressed in the brain (9, 10), suggests that LPL has a novel nonenzymatic function in the brain. However, little is known about LPL function in the brain. Interestingly, it has been shown that LPL is accumulated in senile plaques of Alzheimer disease (AD) brains (11). Moreover, SNPs in the coding region of the LPL gene are associated with disease incidence in clinically diagnosed AD subjects, LPL mRNA expression level, brain cholesterol level, and the severity of AD pathologies, including neurofibrillary tangles and senile plaque density (12). These results suggest that LPL may have a physiological role in the brain, whose alternation is associated with the pathogenesis of AD.

The occurrence of senile plaques in the brain is one of the pathological hallmarks of AD. They contain extracellular deposits of amyloid β protein (Aβ), and the abnormal Aβ deposition or the formation of soluble Aβ oligomers is crucial for AD pathogenesis. Aβ is a physiological peptide whose main species are 40 and 42 amino acids in length, and Aβ42 is the predominant specie in senile plaques (13). The Aβ levels are determined by the balance between its production and degradation/clearance, and an attenuated Aβ catabolism is suggested to cause Aβ accumulation in aging brains (14). Previous studies have shown that astrocytes and microglia directly take up and degrade Aβ42 (15, 16) and that Aβ degradation occurs in late endosomal-lysosomal compartments (17, 18). These lines of evidence, together with the finding that LPL mediates the cellular uptake of lipoproteins (1, 2), led us to carry out experiments to determine whether LPL interacts with Aβ to promote Aβ cellular uptake and degradation in astrocytes. Here, we provide evidence that LPL forms a complex with Aβ and facilitates Aβ cell surface binding and uptake in mouse primary astrocytes through a mechanism that is dependent on heparan sulfate and chondroitin sulfate GAG chains, leading to the lysosomal degradation of Aβ.

MATERIALS AND METHODS

Materials—Bovine LPL, heparinases, and a polyclonal anti-actin antibody were purchased from Sigma. Synthetic Aβ1–42 was purchased from the Peptide Institute (Osaka,

* This work was supported by a grant-in-aid for scientific research on priority areas (Research on Pathomechanisms of Brain Disorders) from the Ministry of Education, Culture, Sports, Science, and Technology of Japan, a grant from the Program for Promotion of Fundamental Studies in Health Sciences of the National Institute of Biomedical Innovation, a grant from the Ministry of Health, Labor, and Welfare of Japan (Research on Dementia, Health, and Labor Sciences Research Grant H20-007), and a grant from the Japan Health Sciences Foundation (Research on Publicly Essential Drugs and Medical Devices).

[S] The on-line version of this article (available at http://www.jbc.org) contains supplemental "Methods" and Fig. 1.

[1] To whom correspondence should be addressed: Department of Alzheimer's Disease Research, National Center for Geriatrics and Gerontology, Gengo 35, Morioka, Obu, Aichi 474-8511, Japan. Tel.: 81-562-46-2311; Fax: 81-562-46-8569; E-mail: michi@ncgg.go.jp.

[2] The abbreviations used are: LPL, lipoprotein lipase; Aβ, amyloid β; ApoE, apolipoprotein E; CS, chondroitin sulfate(s); HS, heparan sulfate; GAG, glycosaminoglycan; ANOVA, one-way analysis of variance.

Japan). Heparin, chondroitin, chondroitin sulfates, and chondroitinase ABC were from Seikagaku (Tokyo, Japan). Monoclonal anti-Aβ antibodies (6E10, 4G8) were purchased from Signet Laboratories (Dedham, MA), and a goat polyclonal anti-ApoE antibody and mouse control IgG were from Millipore (Bedford, MA). An anti-LPL antibody and Cy3- and FITC- conjugated secondary antibodies were purchased from Abcam, Inc. (Cambridge, MA). A monoclonal anti-Aβ antibody (2C8) was purchased from Medical and Biological Laboratories (Nagoya, Japan).

Animals—C57BL/6 mice were purchased from SLC, Inc. (Hamamatsu, Japan). ApoE-KO mice were obtained from Jackson ImmunoResearch Laboratories (Bar Harbor, ME). The National Center of Geriatrics and Gerontology Institutional Animal Care and Use Committee approved the animal studies.

Preparation of LPL—Because the sequence of LPL is highly conserved among mammalian species and the ability of LPL to interact with proteoglycans is also well conserved, we used LPL purified from bovine milk. An LPL suspension (suspended in 3.8 M ammonium sulfate, 0.02 M Tris-HCl, pH 8.0) was centrifuged (10,000 × *g* for 20 min at 4 °C), and the resulting pellet was dissolved in PBS. The prepared LPL was stored at 4 °C and used within 3 days.

Cell Culture—Highly astrocyte-rich cultures were prepared according to a method described previously (19). In brief, brains of postnatal day 2 C57BL/6 mice or ApoE knock-out mice were removed under anesthesia. The cerebral cortices from the mouse brains were dissected, freed from meninges, and diced into small pieces; the cortical fragments were incubated in 0.25% trypsin and 20 mg/ml DNase I in PBS at 37 °C for 20 min. The fragments were then dissociated into single cells by pipetting. The dissociated cells were seeded in 75-cm^2 dishes at a density of 5×10^7 cells per flask in DMEM-containing 10% FBS. After 10 days of incubation *in vitro*, flasks were shaken at 37 °C overnight, and the remaining astrocytes in the monolayer were trypsinized (0.1%) and reseeded. The astrocyte-rich cultures were maintained in DMEM-containing 10% FBS until use.

Assay of Aβ Binding and Uptake in Astrocytes by Western Blotting—Assays were carried out on confluent monolayers of astrocytes grown in 12-well plates. Aβ was dissolved in dimethyl sulfoxide to a final concentration of 1 mM and stored at −40 °C. Aβ (500 nM) and LPL (1–10 μg/ml) were mixed in DMEM. Immediately, the mixture was added to the culture medium of astrocytes. Cells were incubated at 37 °C for 5 h to assess the cellular uptake of Aβ or at 4 °C for 3 h to evaluate the binding of Aβ to the cell surface of astrocytes. In these assays, cells were incubated in serum-free DMEM. After incubation, cells were washed with PBS three times, harvested using a cell scraper and lysed by sonication in radioimmune precipitation assay buffer (1% Nonidet P-40, 0.5% sodium deoxycholate, 0.1% SDS, 150 mM NaCl, 50 mM Tris-HCl (pH 8.0), 1 mM EDTA). Cell lysates were subjected to SDS-PAGE with 4–20% gradient gels (WAKO Pure Chemicals, Osaka, Japan) and transferred to polyvinylidene difluoride membranes (Millipore). Aβ was probed with 6E10 antibody followed by horseradish peroxidase-labeled anti-mouse antibody (Cell Signaling Technology, Inc., Beverly, MA) and chemiluminescent substrate ECL Plus (GE Healthcare). The protein contents of cell lysates were normalized to the expression level of actin protein. To examine the involvement of GAGs, heparin, chemically modified heparins, chondroitin, or chondroitin sulfates (3 μg/ml) were incubated with a mixture solution of Aβ and LPL. Astrocytes were pretreated with a mixture of heparinase II and heparinase III or chondroitinase ABC (0.03 units/ml) for 24 h at 37 °C to evaluate endogenously expressed glycosaminoglycans. Signals were visualized and quantified using a LAS-3000 luminescent image analyzer (Fujifilm, Tokyo, Japan) and ImageJ software (National Institutes of Health, Bethesda, MD). For analyzing protein band densities, a region of interest was drawn around a band, and protein band densities were calculated.

siRNA Interference of LPL—siRNA specific for mouse LPL (sense strand, 5′-CAGCUGAGGACACUUGUCAUCUCAUdTdT-3′; antisense strand, 5′-AUGAGAUGACAAGUGUCCUCAGCUGdTdT-3′) and control siRNA (sense strand, 5′-CAGAGGGCACAUUUGACCUUUCCAUdTdT-3′; antisense strand, 5′-AUGGAAAGGUCAAAUGUGCCCUCUG-3′) was purchased from Invitrogen. Astrocytes grown in 12-well plates for 24 h were transfected with either LPL siRNA or control siRNA with Lipofectamine RNAiMAX (Invitrogen). Forty-eight hours after transfection, cells were treated with Aβ (1 μM) and then incubated at 4 °C for 3 h, and cell-surface associated Aβ was analyzed as described above. An anti-LPL antibody (Gene Tex, Inc.) was used for the detection of LPL.

Assay of Aβ Degradation in Astrocytes—Astrocytes were incubated with Aβ (250 nM) and LPL (2 μg/ml) at 37 °C for 5 h. Subsequently, cells were washed with DMEM and incubated in DMEM for additional hours. Then, Aβ in cell lysates was analyzed by Western blotting as described above.

Immunoprecipitation—Aβ (500 nM) and LPL at various concentrations were incubated in DMEM at 37 °C for 3 h. LPL-Aβ complexes were immunoprecipitated with an anti-LPL antibody and magnetic protein G beads (Dynal, Hamburg, Germany). For detection of LPL-Aβ complexes in the mice brains, brain homogenates from 12-week-old C57BL/6 mice were used. In brief, anesthetized mice were perfused with PBS containing 35 μg/ml heparin for 15 min. The cerebrum was dissected out and homogenized by sonication in 4 volumes of PBS containing a protease inhibitor mixture (P8340; Sigma) and centrifuged at 1,000 × *g* for 10 min at 4 °C. The supernatants were harvested and LPL-Aβ complexes were immunoprecipitated with an anti-LPL antibody and magnetic protein G beads. The obtained precipitates were washed three times with PBS and incubated at 70 °C for 10 min in SDS sample buffer. Dissociated Aβ recovered in the supernatant was assessed by Western blotting as described above. For detection of endogenous Aβ, the supernatants were subjected to SDS-PAGE with 4–20% gradient gels and transferred to polyvinylidene difluoride membranes. The membranes were exposed to microwave irradiation for 20 s, and Aβ was probed with 4G8 antibody followed by horseradish peroxidase-labeled anti-mouse antibody and the chemiluminescent substrate ECL Plus.

Immunocytochemistry—Astrocytes grown on poly-L-lysine-coated coverslips were incubated with a mixture of Aβ (250 nM) and LPL (2 μg/ml) at 37 °C for 5 h. After treatment, the cells were fixed with 4% paraformaldehyde in PBS at room temperature for 10 min, blocked, and permeabilized with 10% normal goat serum and 0.05% saponin in PBS at room temperature for 20 min. In some experiments, cells were washed twice with DMEM followed by incubation at 37 °C for 3 h in DMEM and fixed. The cells were then incubated with primary antibodies followed by Cy3- and FITC-conjugated secondary antibodies. The stained specimens were mounted with Fluor-Save reagents (Calbiochem) and examined under an LSM 510 confocal laser microscope (Carl Zeiss MicroImaging GmbH, Jena, Germany).

Statistical Analysis—The collected data were analyzed by one-way analysis of variance (ANOVA) including appropriate variables followed by the Dunnett's test or unpaired Student's *t* test. Results were considered significant when $p < 0.05$.

RESULTS

LPL Binds to Aβ in Vitro—LPL was incubated with freshly prepared Aβ42 *in vitro*, and the complexes formed were immunoprecipitated with an anti-LPL antibody coupled with magnetic beads, followed by probing Western blots of protein complexes using an anti-Aβ antibody (Fig. 1*A*). Aβ42 was immunoprecipitated with an anti-LPL antibody, but not with control IgG. The levels of Aβ42 recovered in the immunoprecipitates from samples in the presence of 2–5 μg/ml LPL were significantly higher than those from samples in the presence of 0, 0.5, or 1 μg/ml of LPL (Fig. 1, *B* and *C*), suggesting that LPL directly interacts with Aβ42, and these two molecules form a complex in an LPL dose-dependent manner. Furthermore, endogenous mouse Aβ was immunoprecipitated with the anti-LPL antibody from brain homogenates prepared from C57BL/6 mice (Fig. 1*D*), indicating that endogenous mouse LPL directly interacts with endogenous mouse Aβ. We also determined the assembly state of Aβ that forms complex with LPL. Solutions containing Aβ oligomers were subjected to immunoprecipitation/immunoblot analysis, and Aβ42 monomers were immunoprecipitated by an anti-LPL antibody (supplemental Fig. 1).

LPL Promotes Cell Surface Binding and Cellular Uptake of Aβ in Astrocytes—We then determined whether LPL affects the cellular binding of Aβ to astrocytes. Soluble Aβ42 and various concentrations of LPL were added to primarily cultured astrocytes prepared from WT mice and then incubated at 4 °C. LPL (2–5 μg/ml) of significantly augmented Aβ42 binding to astrocytes by 5.8- to 9-fold of that in the case without LPL (Fig. 2, *A* and *B*). To examine the effect of LPL on the cellular uptake of Aβ, we incubated primary astrocytes with soluble Aβ42 at 37 °C for 5 h. Apparently, the level of Aβ uptake by astrocytes increased in the presence of LPL at concentrations of 2 to 5 μg/ml (Fig. 2*C*, lysate). Consistent with the increase in the level of cellular uptake of Aβ, the level of Aβ remaining in culture medium was decreased (Fig. 2*C*, medium). The Aβ levels in the cell lysate quantified are shown in Fig. 2*D*, indicating that Aβ levels were significantly increased by 5–8-fold that in astrocytes incubated without LPL. Next,

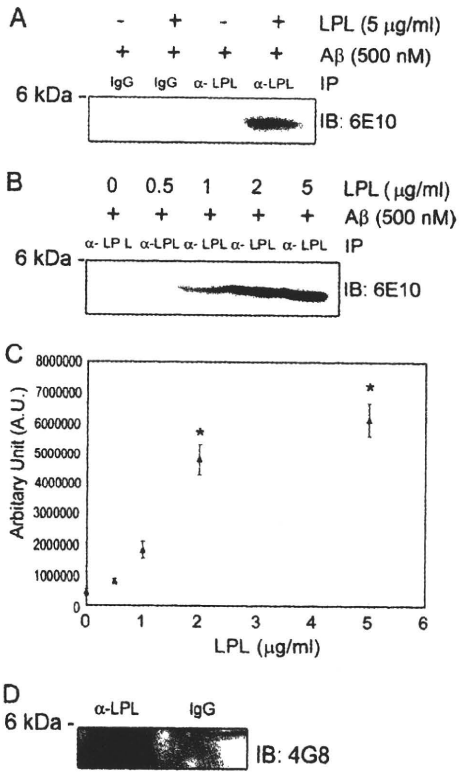

FIGURE 1. **LPL binds to Aβ *in vitro*.** *A*, LPL (5 μg/ml) and Aβ (500 nM) were incubated in DMEM at 37 °C for 3 h. Protein complexes formed were immunoprecipitated with an anti-LPL antibody (α-LPL), and the immunoprecipitates (*IP*) were analyzed by Western blotting using 6E10, an anti-Aβ antibody. These data are representative of three independent experiments. *B*, LPL at various concentrations of 0, 0.5, 1, 2, and 5 μg/ml and Aβ at 500 nM were incubated in DMEM at 37 °C for 3 h. Protein complexes formed were immunoprecipitated with an α-LPL, and the immunoprecipitates were subjected to Western blotting using 6E10. *C*, quantification of Aβ immunoprecipitated with α-LPL. The data presented are the means ± S.D. of three independent experiments. *, $p < 0.001$ *versus* samples without LPL treatment. *D*, the mouse cerebrum was homogenized by sonication in 4 volumes of PBS containing a protease inhibitor mixture and centrifuged at 1000 × *g* for 10 min at 4 °C. The supernatants were harvested. LPL-Aβ complexes in the supernatant were immunoprecipitated with an α-LPL, and the Aβ in the immunoprecipitates was detected by Western blotting using 4G8, an anti-Aβ antibody. *IB*, immunoblot.

we determined the time-dependent effect of LPL-mediated Aβ uptake into astrocytes. Astrocyte cultures were incubated with Aβ (500 nM) and LPL (2 μg/ml) at 37 °C for various hours, and the Aβ level in the cell lysate was determined. The level of Aβ in the cell lysate increased in a time-dependent manner (Fig. 2*E*). The Aβ levels in the astrocytes incubated for 3 and 5 h were significantly higher by 9–14-fold of that in astrocytes incubated without LPL (Fig. 2*F*). These concentrations of LPL are comparable with the concentrations with which LPL could act as "bridging molecules" (2, 20). There were no significant differences among the values for cultures without LPL (one-way ANOVA, $p = 0.1386$). No change in cellular morphology or cell number in astrocyte cultures was observed during the incubation (data not shown). To examine the involvement of LPL expressed by astrocytes, we carried out experiments using the gene silencing technique for LPL. The transient knockdown of LPL expression was achieved by the transfection of siRNA specific for LPL. After transfection,

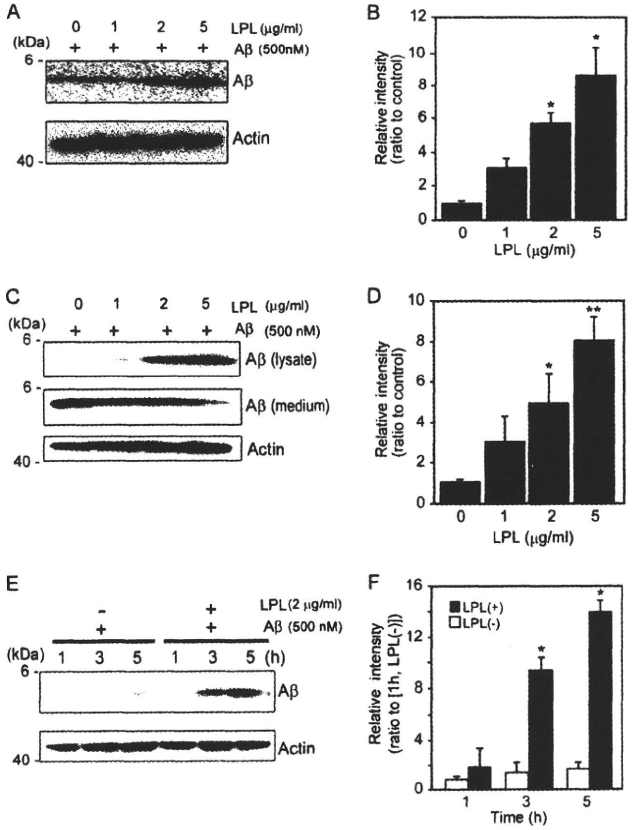

FIGURE 2. **LPL augments cell-surface association and cellular uptake of Aβ in astrocytes.** *A*, mouse primary astrocytes were incubated with LPL (0–5 μg/ml) and Aβ (500 nM) at 4 °C for 3 h. The astrocytes were washed in cold PBS three times, and the cells were harvested using a scraper. The level of Aβ on the cell surface was determined by Western blotting in a detergent extract of whole cells. *B*, quantification of cell-surface-associated Aβ. The data are the means ± S.D. of three independent experiments. *, $p <$ 0.001 *versus* LPL at 0 μg/ml. *C* and *D*, astrocytes were incubated with Aβ (500 nM) and LPL (0, 1, 2, and 5 μg/ml) at 37 °C for 3 h. The cultured cells were then washed thoroughly in PBS for three times, and the cells were collected. The level of Aβ in the whole cell lysate (*lysate*), and the conditioned medium of cultured cells (*medium*) were determined by Western blotting using 6E10 antibody. The level of actin demonstrated by Western blotting using an anti-β-actin antibody was used as the loading control. These data are representative of at least three independent experiments. *D*, quantification of cellular Aβ is shown. The data presented are the means ± S.D. of three independent experiments. *, $p < 0.05$; **, $p < 0.01$ *versus* LPL at 0 μg/ml. *E* and *F*, astrocytes were incubated with Aβ (500 nM) and LPL (2 μg/ml) at 37 °C for 0, 3, and 5 h. The cultured cells were then washed thoroughly in PBS three times, and the cells were collected. The amount of Aβ in the whole cell lysate was determined by Western blotting using 6E10 antibody. The level of actin demonstrated by Western blotting using the anti-β-actin antibody was used as the loading control. These data are representative of at least three independent experiments. *F*, quantification of cellular Aβ is shown. The data are the means ± S.D. of three independent experiments. *, $p < 0.001$ *versus* LPL (+) at 1 h.

cells were treated with Aβ42 (1 μM) and then incubated at 4 °C for 3 h. As shown in Fig. 3, the cellular binding of Aβ42 to astrocytes was significantly decreased by LPL protein knockdown.

Degradation of Internalized Aβ in a Lysosomal Pathway in Astrocytes—Next, we examined the degradation of internalized Aβ. Mouse primary astrocytes were incubated with soluble Aβ42 and LPL at 37 °C for 5 h, washed in DMEM three times, and cultured at 37 °C for additional time (0, 3, 5, 12,

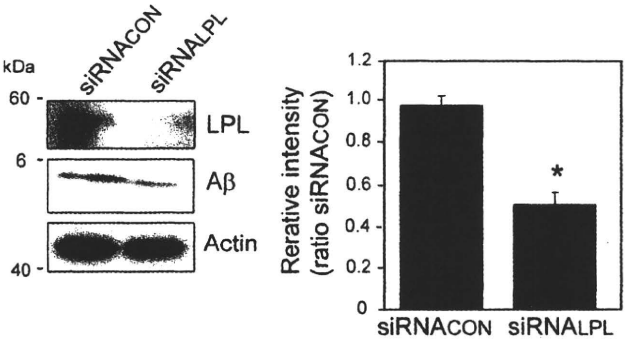

FIGURE 3. **Effect of LPL knockdown on cell-surface association of Aβ in cultured astrocytes.** Astrocytes were transfected with 10 nM siRNA specific for LPL (*siRNALPL*) and control siRNA (*siRNACON*). Forty-eight hours after transfection, cells were treated with Aβ42 (1 μM) at 4 °C for 3 h. The cells were washed in cold PBS three times, and the cells were harvested using a scraper. The level of Aβ42 on the cell surface was determined by Western blotting in a detergent extract of whole cells. The graph shows the levels of cell-surface-associated Aβ. The data are the means ± S.D. of three independent experiments. *, $p < 0.001$ *versus* control siRNA by unpaired Student's *t* test.

and 24 h). Cells were then harvested, and the Aβ level in the cell lysate was analyzed by Western blotting. The strong signal representing internalized Aβ during the initial incubation for 5 h was detected in the cell lysate at the point of 0 min after washing (Fig. 4*A*). Three to five hours after washing, the level of Aβ remaining in the cell lysate partially disappeared (Fig. 4*A*). Twelve and twenty-four hours after washing, the internalized Aβ completely disappeared, indicating that the internalized Aβ was degraded in astrocytes in a time-dependent manner (Fig. 4*A*). To gain insight into the degradation pathway of the internalized Aβ, we investigated the localization of Aβ by immunocytochemical analysis. Mouse primary astrocytes were plated on poly-L-lysine-coated coverglasses and incubated with Aβ42 (500 nM) and LPL (2 μg/ml) at 37 °C for 5 h. In some experiments, cells were washed in DMEM three times and further incubated in serum-free DMEM for 3 h. Cells were then permeabilized and stained with an anti-Aβ antibody, 6E10, and an anti-LAMP2 antibody, whose staining signal is considered as a marker of late endosomes/lysosomes (21). We found that some portions of anti-Aβ antibody-positive signals were co-localized with staining signals reactive to the anti-LAMP2 antibody, showing that the internalized Aβ was trafficked into late endosomal/lysosomal compartments (Fig. 4*B*). To confirm the involvement of a lysosomal pathway in the degradation of LPL-mediated internalized Aβ, we determined the effect of chloroquine on the localization of Aβ internalized in an LPL-mediated manner. Chloroquine is a weak base and is taken up by cells, which results in the neutralization of acidic organelles such as lysosomes and impairment of their functions (22, 23). Chloroquine treatment at concentrations of 25 and 50 μg/ml prevented the degradation of internalized Aβ 12 h after washing out (Fig. 4*C*). We also tested inhibitors of neprilysin, an insulin-degrading enzyme, and cathepsin B, all of which are known to degrade Aβ. These inhibitors failed to suppress the degradation of internalized Aβ in astrocytes (data not shown). Thus, Aβ internalized in an LPL-mediated manner was degraded in a lysosomal pathway in astrocytes.

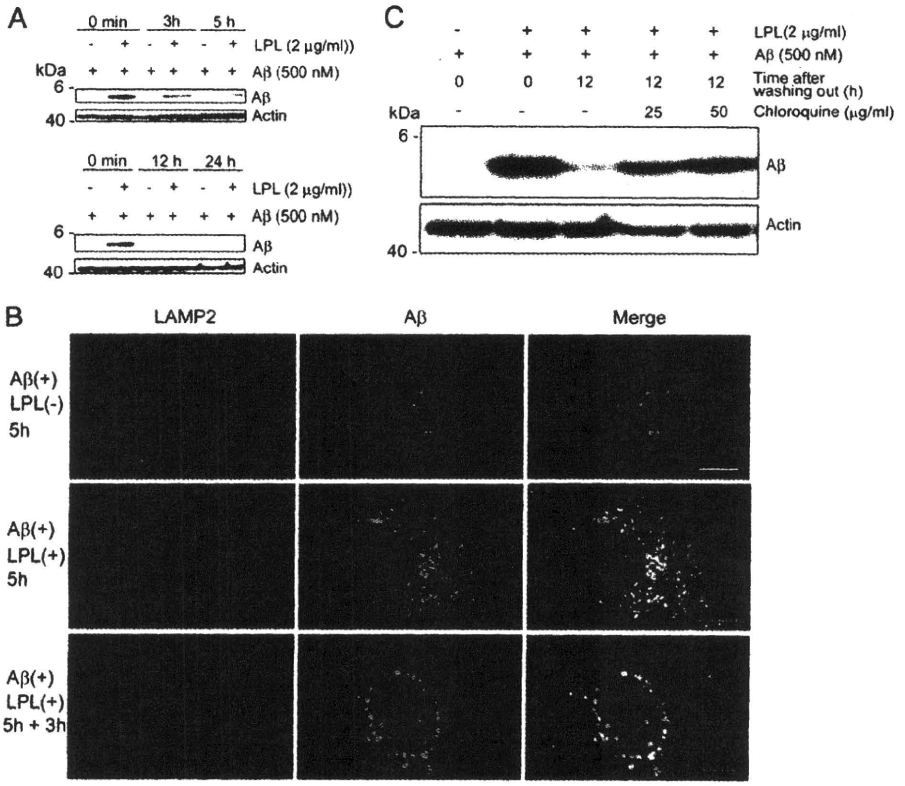

FIGURE 4. **Aβ is trafficked to late endosomal/lysosomal compartments and degraded after the LPL-mediated uptake.** *A*, mouse primary astrocytes were incubated with LPL (2 μg/ml) and Aβ (500 nM) at 37 °C for 5 h. Cells were washed in DMEM three times and then incubated in DMEM at 37 °C for 0, 3, 5, 12, and 24 h. The amount of Aβ remaining in the cells was determined by Western blotting using the anti-Aβ antibody, 6E10, in a detergent extract of whole cells. *B*, astrocytes were plated on poly-L-lysine-coated coverglasses and incubated with LPL (2 μg/ml) and Aβ (250 nM) at 37 °C for 5 h. Then, cells were permeabilized and double stained with an anti-LAMP2 antibody and 2C8. Bound antibodies were visualized with Cy3-conjugated (*red*) and FITC-conjugated (*green*) secondary antibodies for the anti-LAMP2 antibody and 6E10, respectively. Astrocytes incubated without Aβ did not show any anti-Aβ antibody-positive signals (not shown). *Scale bar*, 10 μm. *C*, astrocytes were incubated with LPL (2 μg/ml) and Aβ (500 nM) at 37 °C for 5 h. Cells were then washed in DMEM and cultured with or without chloroquine in DMEM at 37 °C for an additional 12 h. The level of Aβ in the detergent extract of whole cells was determined by Western blotting with 6E10. These are representative data of at least three independent experiments.

LPL Promotes Cellular Uptake of Aβ in a Heparan Sulfate- and Chondroitin Sulfate-dependent Manner—LPL has a high affinity with heparan sulfate (HS) and chondroitin sulfate (CS) (5, 24, 25). Therefore, we next investigated whether HS and CS are involved in the LPL-mediated cellular binding and cellular uptake of Aβ in astrocytes. Mouse primary astrocytes were pretreated with a mixture of heparinase II and heparinase III and/or chondroitinase ABC for 24 h at 37 °C, followed by incubation with Aβ42 and LPL at 4 °C for 3 h. There were no significant differences among the values in the absence of LPL (one-way ANOVA; $p = 0.0929$ for cell-surface-associated Aβ, $p = 0.4350$ for cellular Aβ). Pretreatment with heparinases or chondroitinase ABC partially decreased the level of LPL-mediated cellular binding of Aβ in astrocytes to 40 or 50% of that observed in the nontreated control, respectively (Fig. 5*A*). Interestingly, pretreatment with both heparinases and chondroitinase ABC decreased the level of LPL-mediated binding of Aβ to astrocytes to 20% of that observed in nontreated control (Fig. 5*A*). Next, we determined the effect of HS and/or CS on the LPL-mediated cellular uptake of Aβ. In conjunction with the effect of LPL on Aβ binding, heparinases and chondroitinase ABC decreased the level of LPL-mediated cellular uptake of Aβ in astrocytes to 30 and 50% of that observed in the nontreated control incubated with LPL, respectively (Fig. 5*B*). Pretreatment with both heparinases and chondroitinase ABC did not show an additive effect on the attenuation of LPL-promoted Aβ uptake (Fig. 5*B*). These findings indicate that HS and CS expressed in astrocytes are involved in the LPL-mediated association of Aβ with astrocytes and Aβ cellular uptake.

To further confirm the involvement of HS and CS in LPL-mediated Aβ uptake, we incubated astrocytes with various glycosaminoglycans. Heparin, which is a structural analog of HS, substantially suppressed the effect of LPL on Aβ uptake at a concentration of 3 μg/ml (Fig. 5*C*). The suppressive effect of heparin on LPL-mediated Aβ uptake was also observed in the presence of de-*N*-sulfated heparin, whereas either de-2-*O*-sulfated heparin or de-6-*O*-sulfated heparin had no effect on LPL-mediated Aβ uptake (Fig. 5*C*). None of these heparins interfered with the interaction between LPL and Aβ (Fig. 5*D*). In addition, 4-*O*-, 6-*O*-disulfated chondroitin sulfate (3 μg/ml) completely suppressed the promotive effect of LPL on Aβ uptake (Fig. 5*E*). 4-*O*-Sulfated chondroitin sulfate and 6-*O*-sulfated chondroitin sulfate moderately attenuated the function of LPL, whereas chondroitin (a nonsulfated form of chondroitin sulfate) and 2-*O*-, 6-*O*-disulfated chondroitin

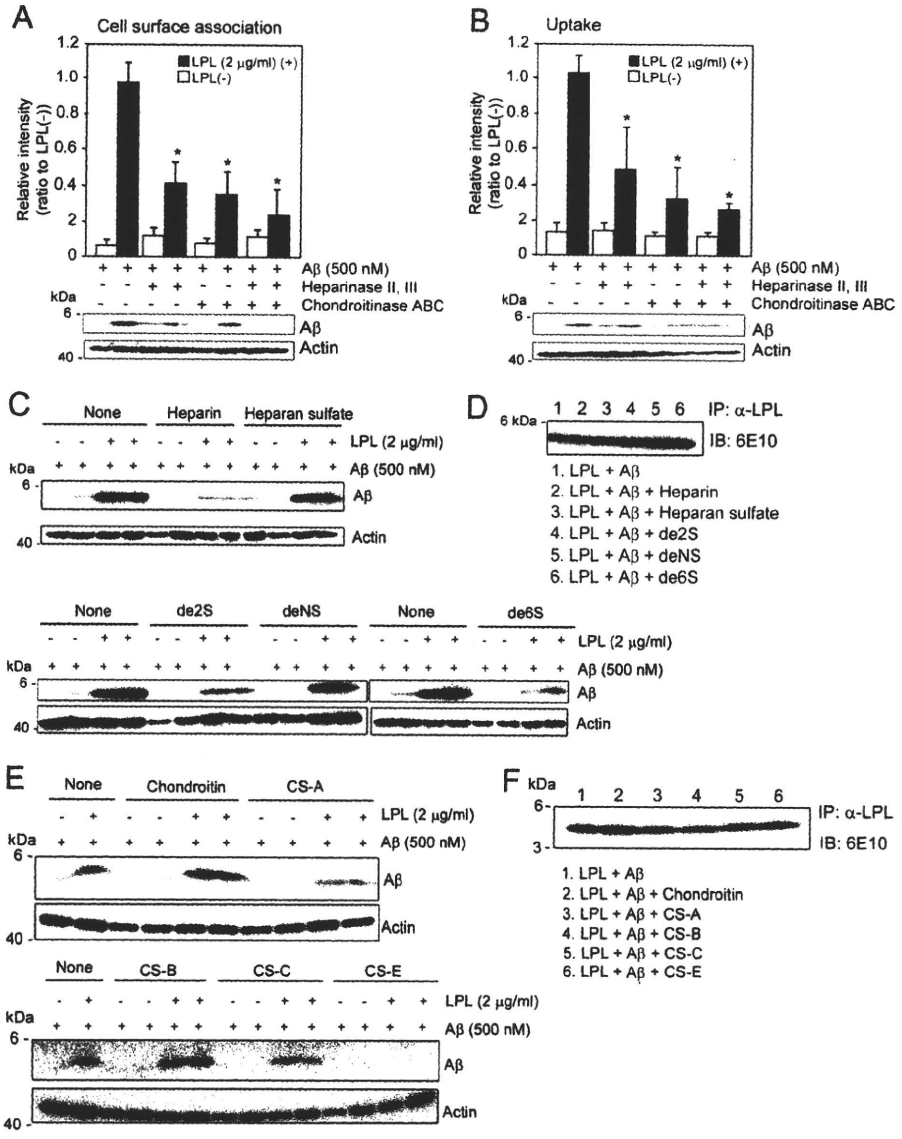

FIGURE 5. **LPL-mediated cellular binding and uptake of Aβ depends on heparan sulfate and chondroitin sulfate in astrocytes.** *A* and *B*, astrocytes from wild-type mice were pretreated with a mixture of heparinase II (0.03 μg/ml) and heparinase III (0.03 μg/ml), and/or chondroitinase ABC (0.03 μg/ml) at 37 °C for 24 h. After washing in DMEM three times, cells were incubated with LPL (2 μg/ml) and Aβ (500 nM) at 4 °C for 3 h (for cell surface association) (*A*) or 37 °C for 3 h (for uptake) (*B*). The level of Aβ in the detergent extract of whole cells was determined by Western blotting using 6E10. The quantitative assessment of cell-surface-associated Aβ (*A*) and cellular Aβ (*B*) in the present (closed bars) or absence (open bars) of LPL are shown. The data presented are the means ± S.D. of three independent experiments. * $p < 0.001$ *versus* levels of LPL (-). (*C*) Mouse primary astrocytes were incubated with Aβ (500 nM) or LPL (2 μg/ml) and Aβ (500 nM) in the presence or absence of heparin or chemically modified heparins at a concentration of 3 μg/ml at 37 °C for 5 h. The level of Aβ in the detergent extract of whole cells was determined using 6E10. (*D*) LPL (2 μg/ml) and Aβ (500 nM) were incubated in DMEM at 37 °C for 3 h in the presence or absence of heparin, heparan sulfate, or chemically modified heparins at a concentration of 3 μg/ml. Protein complexes in DMEM were immunoprecipitated (*IP*) with an anti-LPL antibody (α-LPL) and the Aβ recovered in the immunoprecipitates was analyzed by Western blotting using 6E10. These data are representative of at least three independent experiments. *de2S*, 2-*O*-desulfated heparin; *de6S*, 6-*O*-desulfated heparin; *deNS*, *N*-desulfated heparin. *E*, astrocytes were incubated with LPL (2 μg/ml) and Aβ (500 nM) in the presence or absence of chondroitin sulfates (chondroitin, chondroitin 4-sulfate (*CS-A*), 2-*O*-, 6-*O*-disulfated chondroitin sulfate (*CS-B*), 6-*O*-sulfated chondroitin sulfate (*CS-C*), and chondroitin 4,6-disulfate (*CS-E*)) at a concentration of 3 μg/ml at 37 °C for 5 h. The level of Aβ in a detergent extract of whole cells was determined by Western blotting using 6E10. *F*, LPL (2 μg/ml) and Aβ (500 nM) were incubated in DMEM at 37 °C for 3 h in the presence or absence of chondroitin sulfates at a concentration of 3 μg/ml. Protein complexes were immunoprecipitated with the anti-LPL antibody (α-LPL), and the Aβ recovered in the immunoprecipitates was analyzed by Western blotting using 6E10. The data are representative of at least three independent experiments. *IB*, immunoblot.

sulfate (also known as dermatan sulfate) did not (Fig. 5*E*). None of these CS interfered with the interaction between LPL and Aβ *in vitro* (Fig. 5*F*).

ApoE Is Dispensable for LPL-mediated Cellular Uptake of Aβ in Astrocytes—Because ApoE is reported to be involved in the metabolism of Aβ, including its aggregation and clearance (26), we analyzed the effects of ApoE on the LPL-mediated cellular uptake of Aβ in astrocytes. We collected culture media of primary astrocytes prepared from ApoE-KO mice and C57BL/6 (WT) mice. The astrocyte cultures prepared from wild-type mouse cortices were incubated in conditioned media in the presence of Aβ42 and LPL. As shown in Fig. 6A, Aβ

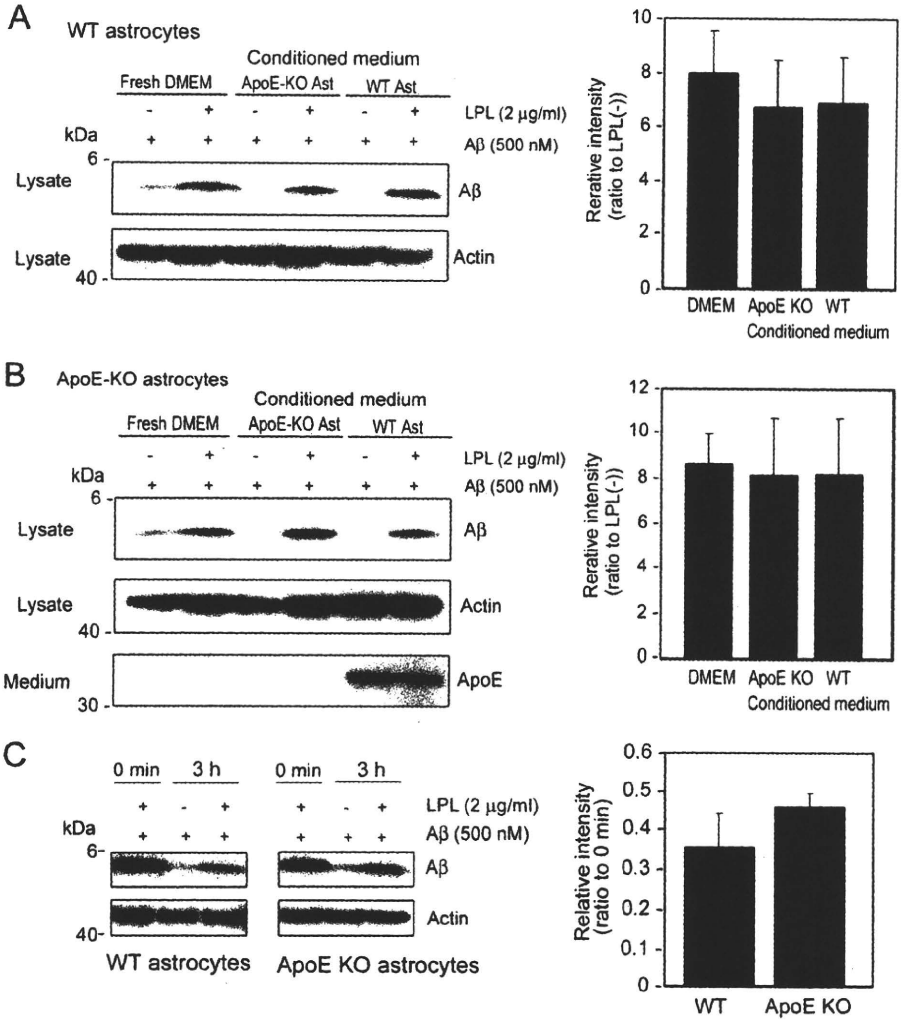

FIGURE 6. **ApoE is dispensable for the LPL-mediated cellular uptake of Aβ in astrocytes.** The astrocyte cultures prepared from WT or ApoE knock-out (KO) mice were incubated in fresh serum-free DMEM for 3 days at 37 °C. The conditioned media of these cultures were then collected. The astrocytes prepared from WT (*A*) or ApoE-KO (*B*) mouse brains were incubated in the conditioned medium of ApoE-KO astrocyte cultures or conditioned medium of WT astrocyte cultures, and LPL (2 μg/ml) and Aβ (500 nM) were added into each culture; the cultures were then maintained for another 5 h at 37 °C. After the incubation, the cultures were harvested, and the amount of cellular Aβ in a detergent extract of whole cells (*lysate*) was determined by Western blotting using 6E10. The amount of ApoE in the conditioned medium of cultured cells (*medium*) was determined by Western blotting using an anti-ApoE antibody, AB947. These data are representative of at least three independent experiments. The graphs show the cellular Aβ levels. The data are the means ± S.D. of three independent experiments. *CM*, conditioned medium; *Ast*, astrocytes. *C*, mouse primary astrocytes from WT and ApoE-KO mice were incubated with soluble Aβ42 in the presence or absence of LPL at 37 °C for 5 h, washed in DMEM three times, and further incubated at 37 °C for 3 h. Cells were then harvested, and the Aβ levels in the lysate was analyzed by Western blotting. The graph shows the cellular Aβ levels. The data are the means ± S.D. of three independent experiments.

uptake was promoted by LPL in astrocytes prepared from WT mice incubated in a fresh medium, the conditioned medium from ApoE-KO astrocytes, and the conditioned medium from WT astrocytes. There were no significant differences between these three groups (one-way ANOVA; $p = 0.6419$). This is also the case for ApoE-KO astrocytes (one-way ANOVA; $p = 0.9467$) (Fig. 6*B*). These findings indicate that ApoE is dispensable for the LPL-promoted cellular uptake of Aβ in astrocytes. We also examined the effects of ApoE on the degradation of internalized Aβ. Primary astrocytes from WT and ApoE-KO mice were incubated with soluble Aβ42 and LPL at 37 °C for 5 h, washed in DMEM three times, and further incubated at 37 °C for 3 h. Cells were then harvested, and the Aβ level in the cell lysate was analyzed by Western blotting. As shown in Fig. 6*C*, there were no significant differences between the levels of Aβ remaining in the lysate of WT astrocytes and ApoE-KO astrocytes ($p = 0.1031$).

DISCUSSION

Previous studies have shown that the mRNA expression of the LPL gene and the enzymatically active LPL are found in the brain in several mammalian species (6, 7, 27). However, considering that the main fraction of lipoproteins in the brain is HDL, which contains negligible or no triacylglycerols, and that the brain lacks an essential cofactor, apoCII, it is conceivable that LPL has a different function in the brain from that in the systemic circulation serving as an enzyme with the cofactor apoCII to catalyze the hydrolysis of triacylglycerols (28). In

the present study, we found a novel function of LPL serving as an Aβ binding molecule; that is, exogenous LPL binds to Aβ and promotes cellular binding and uptake of Aβ in astrocytes. The internalized Aβ was degraded within 12 h, mainly in a lysosomal pathway. Furthermore, we have demonstrated that HS and CS glycosaminoglycans are involved in the promotion of the LPL-mediated cellular uptake of Aβ in astrocytes.

Astrocytes are a major glial cell type in the CNS and play a crucial role in neuronal development, maintenance of synapse functions, and CNS repair after injury. Additionally, astrocytes have phagocytic and proteolytic activities (29, 30) and ingest Aβ (15, 31, 32). Our results indicate that LPL strongly enhances cellular uptake of Aβ, leading to increased degradation of Aβ in astrocytes. Previous studies have shown that SNPs in the coding region of the LPL gene are associated with AD development (33) and the severity of AD pathophysiological features (12), with the molecular mechanisms underlying this association remaining unknown. It may be possible that altered function of LPL shown in this study would result in impaired Aβ clearance and subsequent accumulation of Aβ, accelerating AD development. Because the accumulation of Aβ in the extracellular space is considered to trigger Aβ aggregation and deposition, the function of LPL to enhance Aβ binding, uptake, and degradation in astrocytes may decrease Aβ levels in the brain. However, because LPL is known to regulate the uptake and transport of vitamin E to the brain, of which deficiency results in increased Aβ accumulation and presynaptic defects accompanied by impaired learning and memory function *in vivo* (34, 35), there may be other possibilities as well, that the altered LPL function regulating vitamin E transport may enhance Aβ accumulation and impair synaptic function.

It has been suggested that lysosomal dysfunction plays a major role in Aβ accumulation, thereby causing neuronal cell death (36, 37) and that chloroquine, which disrupts lysosomal pH balance, enhances Aβ accumulation in a microglial cell line (38). Our results show that almost all of the internalized Aβ was localized in lysosomes and degraded in a time-dependent manner, and this degradation was markedly inhibited by the treatment with chloroquine, suggesting that Aβ was degraded mainly in a lysosomal pathway. These findings suggest that lysosomal pathways play a critical role in the degradation of Aβ that is internalized via a novel pathway as LPL-Aβ complexes by astrocytes.

It has been shown that LPL associates with lipoproteins and the formed LPL-bound lipoprotein complexes bind to cell-surface HS proteoglycans and CS proteoglycans (1, 5, 39), promoting the cellular uptake of lipoproteins by acting as a bridging molecule (2, 40). HS proteoglycans and CS proteoglycans are present in astrocytes (41–43). We found that pretreatment of astrocytes with a mixture of heparinases or chondroitinase ABC partially attenuated the LPL-mediated Aβ uptake, and cotreatment with heparinases and chondroitinase ABC completely suppressed the LPL-mediated cellular uptake of Aβ (Fig. 4), indicating that the LPL-mediated cellular uptake of Aβ is mediated via HS proteoglycans and CS proteoglycans. Interestingly, heparin, a highly sulfated form of HS, and 4-*O*-, 6-*O*-disulfated chondroitin sulfate, a highly sulfated CS, selectively suppressed the promotion of Aβ uptake in astrocytes. These findings suggest that LPL could act as a bridging molecule between not only cell-surface GAGs and lipoproteins but also cell-surface GAGs and Aβ and facilitate the cellular uptake of Aβ in astrocytes and that certain domains modified by multiple sulfate groups are necessary for LPL to function in astrocytes.

ApoE is one of the major apolipoproteins in the brain and plays a key role in lipid transport in the brain. ApoE affects the aggregation of Aβ *in vitro* (26). PDAPP and Tg2576 transgenic mice exhibit extensive cerebral Aβ deposition. When these transgenic mice lack the murine *apoE* gene, a significant decrease in amyloid plaque formation was observed (44, 45). Furthermore, two *in vitro* studies have demonstrated that ApoE can facilitate the cellular degradation of Aβ (16, 31). These lines of evidence suggest that ApoE affects Aβ metabolism. Thus, we examined whether ApoE could be involved in the LPL-mediated cellular uptake of Aβ. LPL promoted the cellular uptake of Aβ in wild-type and ApoE-deficient astrocytes in culture. The presence or absence of ApoE in the conditioned medium of astrocytes did not alter the levels of Aβ internalized in an LPL-mediated manner. These results suggest that ApoE is not required for the LPL-mediated cellular uptake of Aβ in astrocytes.

In this study, we demonstrated a novel LPL function; that is, LPL binds to Aβ and enhances the cellular uptake of Aβ in a sulfated glycosaminoglycan-dependent manner, and the internalized Aβ is degraded in a lysosomal pathway. Although further studies will be needed to confirm the role of LPL in the clearance of Aβ *in vivo*, our findings provide a new insight into the molecular pathogenesis of AD and a potential strategy for AD therapy.

REFERENCES

1. Williams, K. J., Fless, G. M., Petrie, K. A., Snyder, M. L., Brocia, R. W., and Swenson, T. L. (1992) *J. Biol. Chem.* **267,** 13284–13292
2. Mulder, M., Lombardi, P., Jansen, H., van Berkel, T. J., Frants, R. R., and Havekes, L. M. (1993) *J. Biol. Chem.* **268,** 9369–9375
3. Kreuger, J., Spillmann, D., Li, J. P., and Lindahl, U. (2006) *J. Cell Biol.* **174,** 323–327
4. Edwards, I. J., Goldberg, I. J., Parks, J. S., Xu, H., and Wagner, W. D. (1993) *J. Lipid Res.* **34,** 1155–1163
5. Edwards, I. J., Xu, H., Obunike, J. C., Goldberg, I. J., and Wagner, W. D. (1995) *Arterioscler. Thromb. Vasc. Biol.* **15,** 400–409
6. Goldberg, I. J., Soprano, D. R., Wyatt, M. L., Vanni, T. M., Kirchgessner, T. G., and Schotz, M. C. (1989) *J. Lipid Res.* **30,** 1569–1577
7. Yacoub, L. K., Vanni, T. M., and Goldberg, I. J. (1990) *J. Lipid Res.* **31,** 1845–1852
8. Eckel, R. H., and Robbins, R. J. (1984) *Proc. Natl. Acad. Sci. U.S.A.* **81,** 7604–7607
9. Havel, R. J., Fielding, C. J., Olivecrona, T., Shore, V. G., Fielding, P. E., and Egelrud, T. (1973) *Biochemistry* **12,** 1828–1833
10. Zannis, V. I., Cole, F. S., Jackson, C. L., Kurnit, D. M., and Karathanasis, S. K. (1985) *Biochemistry* **24,** 4450–4455
11. Rebeck, G. W., Harr, S. D., Strickland, D. K., and Hyman, B. T. (1995) *Ann. Neurol.* **37,** 211–217
12. Blain, J. F., Aumont, N., Théroux, L., Dea, D., and Poirier, J. (2006) *Eur. J. Neurosci.* **24,** 1245–1251
13. Iwatsubo, T., Odaka, A., Suzuki, N., Mizusawa, H., Nukina, N., and Ihara, Y. (1994) *Neuron* **13,** 45–53
14. Tanzi, R. E., Moir, R. D., and Wagner, S. L. (2004) *Neuron* **43,** 605–608
15. Wyss-Coray, T., Loike, J. D., Brionne, T. C., Lu, E., Anankov, R., Yan, F.,

Silverstein, S. C., and Husemann, J. (2003) *Nat. Med.* **9,** 453–457
16. Jiang, Q., Lee, C. Y., Mandrekar, S., Wilkinson, B., Cramer, P., Zelcer, N., Mann, K., Lamb, B., Willson, T. M., Collins, J. L., Richardson, J. C., Smith, J. D., Comery, T. A., Riddell, D., Holtzman, D. M., Tontonoz, P., and Landreth, G. E. (2008) *Neuron* **58,** 681–693
17. Majumdar, A., Cruz, D., Asamoah, N., Buxbaum, A., Sohar, I., Lobel, P., and Maxfield, F. R. (2007) *Mol. Biol. Cell* **18,** 1490–1496
18. Mandrekar, S., Jiang, Q., Lee, C. Y., Koenigsknecht-Talboo, J., Holtzman, D. M., and Landreth, G. E. (2009) *J. Neurosci.* **29,** 4252–4262
19. Michikawa, M., Gong, J. S., Fan, Q. W., Sawamura, N., and Yanagisawa, K. (2001) *J Neurosci.* **21,** 7226–7235
20. Fernández-Borja, M., Bellido, D., Vilella, E., Olivecrona, G., and Vilaró, S. (1996) *J. Lipid Res.* **37,** 464–481
21. Fukuda, M. (1991) *J. Biol. Chem.* **266,** 21327–21330
22. de Duve, C., de Barsy, T., Poole, B., Trouet, A., Tulkens, P., and Van Hoof, F. (1974) *Biochem. Pharmacol.* **23,** 2495–2531
23. Poole, B., and Ohkuma, S. (1981) *J. Cell Biol.* **90,** 665–669
24. Bengtsson, G., Olivecrona, T., Höök, M., Riesenfeld, J., and Lindahl, U. (1980) *Biochem. J.* **189,** 625–633
25. Pillarisetti, S., Paka, L., Sasaki, A., Vanni-Reyes, T., Yin, B., Parthasarathy, N., Wagner, W. D., and Goldberg, I. J. (1997) *J. Biol. Chem.* **272,** 15753–15759
26. Kim, J., Basak, J. M., and Holtzman, D. M. (2009) *Neuron* **63,** 287–303
27. Brecher, P., and Kuan, H. T. (1979) *J. Lipid Res.* **20,** 464–471
28. Koch, S., Donarski, N., Goetze, K., Kreckel, M., Stuerenburg, H. J., Buhmann, C., and Beisiegel, U. (2001) *J. Lipid Res.* **42,** 1143–1151
29. al-Ali, S. Y., and al-Hussain, S. M. (1996) *J. Anat.* **188,** 257–262
30. Hatten, M. E., Liem, R. K., Shelanski, M. L., and Mason, C. A. (1991) *Glia* **4,** 233–243
31. Koistinaho, M., Lin, S., Wu, X., Esterman, M., Koger, D., Hanson, J., Higgs, R., Liu, F., Malkani, S., Bales, K. R., and Paul, S. M. (2004) *Nat. Med.* **10,** 719–726
32. Matsunaga, W., Shirokawa, T., and Isobe, K. (2003) *Neurosci. Lett.* **342,** 129–131
33. Baum, L., Chen, L., Masliah, E., Chan, Y. S., Ng, H. K., and Pang, C. P. (1999) *Am. J. Med. Genet.* **88,** 136–139
34. Xian, X., Liu, T., Yu, J., Wang, Y., Miao, Y., Zhang, J., Yu, Y., Ross, C., Karasinska, J. M., Hayden, M. R., Liu, G., and Chui, D. (2009) *J. Neurosci.* **29,** 4681–4685
35. Nishida, Y., Ito, S., Ohtsuki, S., Yamamoto, N., Takahashi, T., Iwata, N., Jishage, K., Yamada, H., Sasaguri, H., Yokota, S., Piao, W., Tomimitsu, H., Saido, T. C., Yanagisawa, K., Terasaki, T., Mizusawa, H., and Yokota, T. (2009) *J. Biol. Chem.* **284,** 33400–33408
36. Bahr, B. A., and Bendiske, J. (2002) *J Neurochem.* **83,** 481–489
37. Nixon, R. A., Cataldo, A. M., and Mathews, P. M. (2000) *Neurochem. Res.* **25,** 1161–1172
38. Chu, T., Tran, T., Yang, F., Beech, W., Cole, G. M., and Frautschy, S. A. (1998) *FEBS Lett.* **436,** 439–444
39. Eisenberg, S., Sehayek, E., Olivecrona, T., and Vlodavsky, I. (1992) *J. Clin. Invest.* **90,** 2013–2021
40. Auerbach, B. J., Bisgaier, C. L., Wölle, J., and Saxena, U. (1996) *J. Biol. Chem.* **271,** 1329–1335
41. Hsueh, Y. P., and Sheng, M. (1999) *J. Neurosci.* **19,** 7415–7425
42. Laabs, T. L., Wang, H., Katagiri, Y., McCann, T., Fawcett, J. W., and Geller, H. M. (2007) *J. Neurosci.* **27,** 14494–14501
43. Tsuchida, K., Shioi, J., Yamada, S., Boghosian, G., Wu, A., Cai, H., Sugahara, K., and Robakis, N. K. (2001) *J. Biol. Chem.* **276,** 37155–37160
44. Bales, K. R., Verina, T., Dodel, R. C., Du, Y., Altstiel, L., Bender, M., Hyslop, P., Johnstone, E. M., Little, S. P., Cummins, D. J., Piccardo, P., Ghetti, B., and Paul, S. M. (1997) *Nat. Genet.* **17,** 263–264
45. Holtzman, D. M., Bales, K. R., Wu, S., Bhat, P., Parsadanian, M., Fagan, A. M., Chang, L. K., Sun, Y., and Paul, S. M. (1999) *J. Clin. Invest.* **103,** R15–R21